

# Schrödinger method as N-body double and UV completion of dust

Cora Uhlemann,<sup>1,2</sup> Michael Kopp,<sup>1,2,3</sup> and Thomas Haugg<sup>1</sup>

<sup>1</sup>*Arnold Sommerfeld Center for Theoretical Physics, Ludwig-Maximilians-Universität, Theresienstr. 37, 80333 Munich, Germany*

<sup>2</sup>*Excellence Cluster Universe, Boltzmannstr. 2, 85748 Garching, Germany*

<sup>3</sup>*University Observatory, Ludwig-Maximilians University, Scheinerstr. 1, 81679 Munich, Germany*

We investigate large scale structure formation of collisionless dark matter in the phase-space description based on the Vlasov (or collisionless Boltzmann) equation whose nonlinearity is induced solely by gravitational interaction according to the Poisson equation. Determining the time-evolution of density and peculiar velocity demands solving the full Vlasov hierarchy for the moments of the phase-space distribution function. In the presence of long-range interaction no consistent truncation of the hierarchy is known apart from the pressureless fluid (dust) model which is incapable of describing virialization due to the occurrence of shell-crossing singularities and the inability to generate vorticity and higher cumulants like velocity dispersion. Our goal is to find a phase-space distribution function that is able to describe regions of multi-streaming and therefore can serve as theoretical N-body double. We use the coarse-grained Wigner probability distribution obtained from a wavefunction fulfilling the Schrödinger-Poisson equation (SPE) and show that its evolution equation bears strong resemblance to the Vlasov equation but cures the shell-crossing singularities. This feature was already employed in cosmological simulations of large-scale structure formation by Widrow & Kaiser (1993). The coarse-grained Wigner ansatz allows to calculate all higher moments from density and velocity analytically thereby incorporating nonzero higher cumulants in a self-consistent manner. On this basis we are able to show that the Schrödinger method (ScM) automatically closes the corresponding hierarchy such that it suffices to solve the SPE in order to directly determine density and velocity and thereby all higher cumulants.

## I. INTRODUCTION

The standard model of large-scale structure (LSS) formation and halo formation is based on collisionless cold dark matter (CDM), a yet unknown particle species that for purposes of LSS and halos can be assumed to interact only gravitationally and to be cold or initially single-streaming. We are therefore interested in the dynamics of a large collection of identical point particles that via gravitational instability evolve from initially small density perturbations into eventually bound structures, like halos that are distributed along the loosely bound LSS composed of superclusters, sheets, and filaments [1–3]. All these structures depend on cosmological parameters, in particular the background energy density of CDM and the cosmological constant during the various epochs we can observe. We therefore require accurate modeling and theoretical understanding of CDM dynamics. While the shape of the LSS can be reasonably well described by modeling the CDM as a pressureless fluid (dust), it necessarily fails at small scales where multiple streams form. Multi-streaming is especially important for halo formation – virialisation, but already affects LSS and its observation in redshift-space.

On sub-Hubble scales and for non-relativistic velocities the Newtonian limit of the Einstein equations is sufficient in order to describe the time evolution of structures within the universe [4–6]. Furthermore the large number of particles under consideration suppresses collisions such that the phase-space dynamics is only affected by the smooth Newtonian gravitational potential [7]. Therefore the time-evolution of the phase-space distribution function  $f(t, \mathbf{x}, \mathbf{p})$  is governed by the Vlasov (or collisionless Boltzmann) equation whose nonlinearity is induced by the gravitational force calculated from the Poisson equation.

Even though this model seems to be quite simple from a conceptual point of view, no general solution is known and

one usually has to resort to N-body simulations which tackle the problem of solving the dynamical equations numerically, see [2, 8–12]. From the analytical point of view, different methods to describe LSS formation based on the dust model have been developed. The dust model describes CDM as a pressureless fluid using hydrodynamic equations [1], and is studied especially in the context of perturbation theory. Among them the two most commonly used methods are the Eulerian framework describing the dynamics of density and velocity fields, see [13], and the Lagrangian description following the field of trajectories of particles [14]. The dust model is an exact solution to the Vlasov equation and describes absolutely cold dark matter and works quite well in the linear and quasi-linear regime of LSS formation. But the dust model not only fails to catch the dynamics when multiple streams occur in the N-body dynamics, but actually runs into so called shell-crossing singularities or caustics forming at the smallest scales. One might therefore say that the dust model is UV-incomplete.

A possibility to circumvent the formation of pancake singularities and to restore agreement with simulations in the weakly nonlinear regime is to introduce an artificial viscosity term in the pressureless fluid equations which is effective only in regions where the dust evolution would predict a singularity. This phenomenological model proposed in [15] is known as adhesion approximation and was shown to be able to reproduce the skeleton of the cosmic web in [16]. However, such ad-hoc constructions remain quite unsatisfying from a conceptual point of view; for example the size of formed structures directly depends on the viscosity parameter rather than the initial conditions.

A more general reasoning was pursued in the direction of coarse-grained perturbation theory which led to models that naturally incorporate adhesive features. When the

dynamical evolution of a many-body system is described by means of a continuous phase-space distribution one has to consider coarse-grained or macroscopic quantities thereby neglecting detailed information about the microscopic degrees of freedom. Although at a first glance this might seem inconvenient, it is indeed an advantageous point of view, especially when comparing to data inferred from observations or simulations, that are fundamentally coarse grained. Therefore the dynamical evolution of smoothed density and velocity fields relevant for cosmological structure formation has been under investigation, see for example [17, 18] where it was illustrated that coarse-graining leads automatically to adhesive behavior. Furthermore it was shown in [19] that for averaged fields the correspondence between the occurrence of velocity dispersion and multi-streaming phenomena due to shell-crossing breaks down. This is due to the fact that the coarse-graining introduces a nonzero velocity dispersion between the particles within each coarse-graining cell which mimics microscopic velocity dispersion connected to genuine multi-streaming.

Solving the Vlasov equation is equivalent to solving the infinite coupled hierarchy of equations for the moments of the distribution function  $f$  with respect to momentum  $\mathbf{p}$ . This means that in order to determine the time evolution of the first two moments, density and velocity, all higher cumulants starting with velocity dispersion are relevant, see [20]. Only neglecting them entirely is consistent [20]; in this case one is lead to the popular dust model [1]. Since gravity is the dominant force on cosmological scales and in the early stages of gravitational instability matter is distributed very smoothly with nearly single-valued velocities, the dust model has proven quite successful in describing the evolution as long as the collective motion of particles is well-described by a coherent flow. However, as soon as the density contrast becomes non-linear, multiple streams become relevant and sheet-like caustics – called ‘shell-crossing’ singularities or Zel’dovich pancakes – are developed indicating that the underlying approximations are no longer justified and the model loses its predictability. The problem of developing singularities and failure of being a good description afterwards, also occurs in the first order Lagrangian solution, called Zel’dovich approximation [21], which is the exact solution in the plane-parallel collapse studied in Sec. IV.

The Schrödinger method (ScM), originally proposed in [22, 23] as numerical technique for following the evolution of CDM, models CDM as a complex scalar field obeying the coupled Schrödinger-Poisson equations (SPE) [24–26] in which  $\hbar$  merely is a free parameter that can be chosen at will and determines the phase space resolution. ScM is comprised of two parts; (1) solving the SPE with desired initial conditions and (2) taking the Husimi transform [27] to construct a phase space distribution from the wave function. The correspondence between distribution functions in classical mechanics and phase-space representations of quantum mechanics has been investigated in detail by [28], both analytically as well as by means of numerical examples. It turned out that the pure Wigner function, obtained from

a wave function fulfilling the SPE, corresponds poorly to classical dynamics. In contrast, the coarse grained Wigner or Husimi distribution was shown to be indeed a good model for coarse grained classical mechanics [22, 28].

The SPE can be seen as the non-relativistic limit of the Klein-Gordon-Einstein equations [29, 30]. From this perspective the physical interpretation (if  $\hbar$  takes the value of the actual Planck constant) is that CDM is actually a non-interacting and non-relativistic Bose-Einstein condensate in which case the SPE can be interpreted as a special Gross-Pitaevskii equation, see [31] for a review. In plasma and solid state physics as well as mathematical physics the equation is known as Choquard equation [32, 33]. In the context of gravitational state reduction the equation was studied under the name Schrödinger-Newton equation, for instance [34]. There have also been investigations on the connection between general fluid dynamics and wave mechanics, see for instance [35, 36].

The similarity between the SPE and the dust model has been also employed in the context of wave mechanics where the so-called free-particle approximation (based on the free-particle Schrödinger equation, see [37]) was shown to closely resemble the Zeldovich approximation [24, 25] avoiding singularities. In some works a modified SPE system with an added quantum pressure term was considered, [38, 39] which then is equivalent to the usual fluid system. Clearly this approach is not advantageous since the fluid description is known to break down at shell-crossing. This had lead to the claim in [38] that also this modified Schrödinger breaks down.

That the ScM is a viable model for cosmological structure formation and in particular capable of describing multi-streaming was exemplarily demonstrated by means of numerical examples in [22, 23, 40]. However, the bulk of these investigations were aimed at replacing N-body simulations by a numerical solution to the SPE. Therefore the methods applied therein are unsuitable and inconvenient for a genuine analytical approach we want to establish. In [22, 23] a superposition of  $N$  Gaussian wave packets was used as initial wave function, thereby closely resembling the  $N$  particles in a N-body simulation. In [40] CDM was modelled by  $N$  wave functions coupled via the Poisson equation. We will study the case of a single wave function on an expanding background with nearly cold initial conditions. The result suggests that indeed the ScM is a substantially better suited analytical tool to study CDM dynamics than the dust model: in the single stream regime they stay arbitrarily close to each other, but while dust fails and stops when multi streaming should occur, the Schrödinger wave function continues without any pathologies and behaves like multi-streaming CDM when interpreted in a coarse-grained sense. Although it was already observed in [24] that the wave function does not run into singularities, it was claimed that it still cannot describe multi-streaming or virialisation. Indeed, our numerical example closely resembling that of [24], but generalised to an expanding background, proves the contrary. Fig 1 shows the dynamics of the Husimi function  $f_H$  using the ScM: the density remains finite at shell crossing,  $f_H$  forms multi-stream regions and ultimately

virialises. None of these features crucial for LSS are accessible with the dust model.

**Goal** The aim of this paper is to present the Schrödinger method, already investigated in the context of cosmological simulations, as a theoretical N-body double for the phase space distribution function  $f$ . We show that phase space density  $f_H$  obtained from ScM solves the Vlasov equation approximately but in a controlled manner. We demonstrate that  $f_H$  closes the hierarchy of moments automatically but yet allows for multi-streaming and virialisation. We give explicit analytic expressions for higher order non-vanishing cumulants, like velocity dispersion, in terms of the wave function and in terms of the macroscopic physical density and velocity fields. This constitutes a new approach to tackle the closure problem of the Vlasov hierarchy apart from truncation or restricting oneself to the dust model and its limitations. We shed light on the physical interpretation by means of a numerical study of pancake formation. In summary this means that the ScM models CDM in a well-behaved manner with initial conditions arbitrarily close to dust. Unlike dust, the ScM captures all relevant physics for describing CDM dynamics even in the deeply nonlinear regime and won't fail on the smallest scales therefore providing an UV-completion of dust.

**Structure** This paper is organized as follows: In Sec. II we review the phase-space description of cold dark matter and explain how one is lead to the Vlasov equation on an expanding background. After introducing the dust model we re-derive the coarse-grained Vlasov equation. We then introduce the Wigner function as an ansatz for the phase-space distribution and explain its connection to the dust model. We derive the corresponding Wigner-Vlasov equation as well as its coarse-grained version and discuss their relations to the usual and the coarse-grained Vlasov equation, respectively. In Sec. III we determine the moments of the three different phase space distributions – the dust model, the Wigner function and the coarse-grained Wigner or Husimi distribution. In Sec. IV we investigate the pancake collapse to illustrate that the dynamics of the complex scalar field is free from the pathologies of the dust fluid and serves therefore both as a theoretical N-body double and as a UV completion of dust. On this basis we explain how the closure of the hierarchy of moments can be achieved and finally discuss the implications. In Sec. V we make suggestions about possible future research based on ScM and conclude in Sec. VI.

## II. PHASE-SPACE DESCRIPTION OF COLD DARK MATTER

### A. From Klimontovich to Vlasov equation

The exact  $N$ -particle (Klimontovich) phase space density  $f_K$  of  $N$  identical particles following trajectories  $\{\mathbf{x}_i(t), \mathbf{p}_i(t)\}$ ,  $i \in 1, \dots, N$ , in phase space is given by a sum of  $\delta$ -functions

$$f_K(t, \mathbf{x}, \mathbf{p}) = \frac{1}{N} \sum_{i=1}^N \delta_D(\mathbf{x} - \mathbf{x}_i(t)) \delta_D(\mathbf{p} - \mathbf{p}_i(t)). \quad (1)$$

We use comoving coordinates  $\mathbf{x}$  with associated conjugate momentum  $\mathbf{p} = a^2 m d\mathbf{x}/dt$ , where  $a$  is the scale factor satisfying the Friedmann equation of a  $\Lambda$ CDM or Einstein-de Sitter universe.<sup>1</sup> For convenience we will in general suppress the  $t$ -dependence of the distribution function in the following. This phase space density obeys the Klimontovich equation [41] encoding phase space density conservation along phase-space trajectories

$$\frac{Df_K}{dt} = \frac{\partial f_K}{\partial t} + \frac{d\mathbf{x}}{dt} \cdot \frac{\partial f_K}{\partial \mathbf{x}} + \frac{d\mathbf{p}}{dt} \cdot \frac{\partial f_K}{\partial \mathbf{p}} = 0. \quad (2)$$

Upon using the equations of motion for non-relativistic particles on trajectories  $\{\mathbf{x}_i(t), \mathbf{p}_i(t)\}$  one arrives at

$$\partial_t f_K = -\frac{\mathbf{p}}{a^2 m} \cdot \nabla_{\mathbf{x}} f_K + m \nabla_{\mathbf{x}} V \cdot \nabla_{\mathbf{p}} f_K. \quad (3a)$$

The nonlinearity in (3a) is induced by the fact that the Newtonian potential  $V$  describes gravitational interaction and therefore depends through Poisson's equation on the density field given by the integral of the distribution function over momentum

$$\Delta V = \frac{4\pi G \rho_0}{a} \left( \int d^3 p f_K - 1 \right), \quad (3b)$$

where  $\rho_0$  is the (constant) comoving matter background density such that  $f_K$  has background value or spatial average value  $\langle \int d^3 p f_K \rangle_{\text{vol}} = 1$ . A  $\nabla$  or  $\Delta = \nabla \cdot \nabla$  means  $\nabla_{\mathbf{x}}$  or  $\Delta_{\mathbf{x}}$ , respectively.

Retaining all details concerning the microstate of a system, the Klimontovich density is not really of practical use. Rather one is interested in the statistical average taken over an ensemble of different realizations of the distribution of the  $N$  particles. This information is contained within the one-particle phase space density  $f_1$  given by

$$f_1(t, \mathbf{x}, \mathbf{p}) = \langle f_K(t, \mathbf{x}, \mathbf{p}) \rangle, \quad (4)$$

where angle brackets denote the ensemble average. If  $V$  was a specified external potential,  $f_1$  would obey the same equation as  $f_K$ . However, since  $V$  is the gravitational potential computed self-consistently from the particles via (3b), the  $\nabla_{\mathbf{x}} V \cdot \nabla_{\mathbf{p}} f_K$  term in (3a) is quadratic in  $f_K$ . Therefore when taking the ensemble average to derive an equation for the one-particle distribution function  $f_1$  an additional correlation term emerges which involves the irreducible part  $f_{2c}$  of two-particle distribution function  $f_2(\mathbf{x}, \mathbf{p}, \mathbf{x}', \mathbf{p}') = f_1(\mathbf{x}, \mathbf{p}) f_1(\mathbf{x}', \mathbf{p}') + f_{2c}(\mathbf{x}, \mathbf{p}, \mathbf{x}', \mathbf{p}')$ , compare [42]

$$\begin{aligned} \partial_t f_1 = & -\frac{\mathbf{p}}{a^2 m} \cdot \nabla_{\mathbf{x}} f_1 + m \nabla_{\mathbf{x}} V \cdot \nabla_{\mathbf{p}} f_1 \\ & + m \int d^3 x' d^3 p' \nabla_{\mathbf{x}} V(\mathbf{x} - \mathbf{x}') \cdot \nabla_{\mathbf{p}} f_{2c}(\mathbf{x}, \mathbf{p}, \mathbf{x}', \mathbf{p}'). \end{aligned} \quad (5)$$

<sup>1</sup> More generally, any expansion history is allowed as long as metric perturbations are only sourced by CDM.

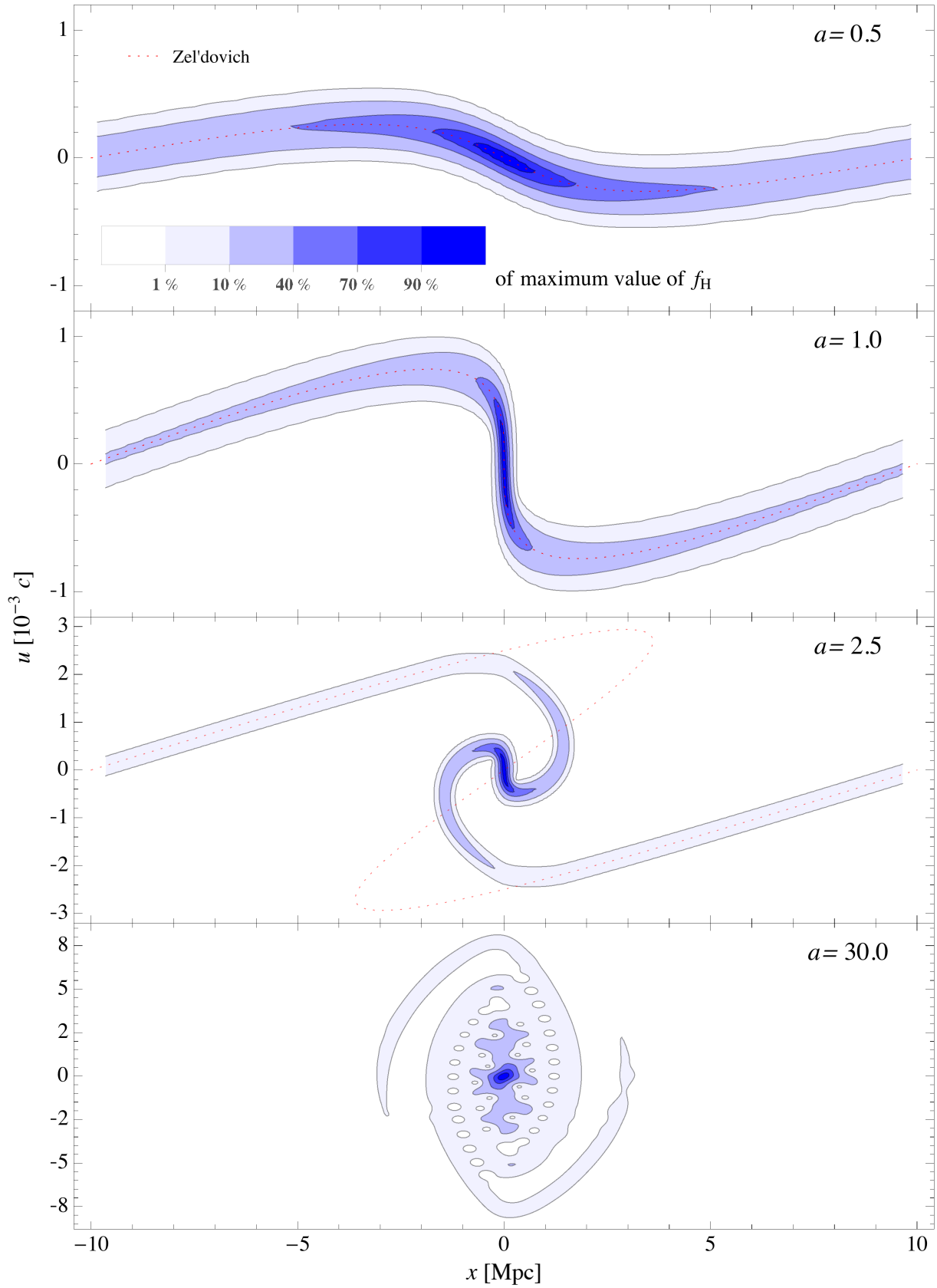


FIG. 1. Collapse of a pancake (plane-parallel) density profile on an Einstein-de Sitter background as seen in phase space using the ScM. *blue* contours: Phase space density  $f_H$  calculated from Eqs. (13, 23) at four moments in time. *red dotted* line: the Zel'dovich solution of Eq. (B3) is the exact dust solution, valid until  $a = 1$ . Only the first panel of the four characteristic moments can be described by dust. Shell crossing (2nd panel), multi-streaming (3rd panel) and virialisation (4th panel) are accessible with the ScM but not with dust. That the dynamics corresponds to CDM is proven in Sec. IID. How to obtain cumulants without constructing  $f_H$  is shown in Sec. IIIC.

This leads to a set of coupled kinetic equations where the  $n$ -particle distribution in turn depends on the  $(n+1)$ -particle distribution. This is the so-called BBGKY (Bogoliubov-Born-Green-Kirkwood-Yvon) hierarchy, describing the dynamics of an interacting  $N$ -particle system. The resulting equation (5) for  $f_1$  differs from the Klimontovich equation (3) by a correlation term which vanishes in the absence of pair correlations. Fortunately, for the case of interest here - CDM particles - these collisional effects are completely negligible since they are suppressed by  $1/N$  where  $N$  is the number of particles, see [7]. The corresponding Vlasov-Poisson system for the one-particle phase space density  $f_1$ , which we will denote simply by  $f$  from now on, describes collisionless dark matter in the absence of two-body correlations

$$\partial_t f = -\frac{\mathbf{p}}{a^2 m} \cdot \nabla_x f + m \nabla_x V \cdot \nabla_p f, \quad (6a)$$

$$= \left[ \frac{\mathbf{p}^2}{2a^2 m} + mV(\mathbf{x}) \right] \left( \overleftarrow{\nabla}_x \overrightarrow{\nabla}_p - \overleftarrow{\nabla}_p \overrightarrow{\nabla}_x \right) f, \quad (6b)$$

$$\Delta V = \frac{4\pi G \rho_0}{a} \left( \int d^3 p f - 1 \right). \quad (6c)$$

### B. Dust model

The dust model describes CDM as a pressureless fluid with density  $n(\mathbf{x})$  and fluid momentum given by an irrotational flow  $\nabla \phi(\mathbf{x})$  which remains single valued at each point, and therefore absolutely cold, meaning that particle trajectories are not allowed to cross and velocity dispersion cannot arise. This regime is usually referred to as ‘single stream’ meaning that the validity of this model breaks down as soon as ‘shell-crossings’ occur and multiple streams develop. The corresponding distribution function is given by

$$f_d(\mathbf{x}, \mathbf{p}) = n(\mathbf{x}) \delta(\mathbf{p} - \nabla \phi(\mathbf{x})). \quad (7)$$

As we will see in section III, the Vlasov equation (6a) for  $f_d$  implies the hydrodynamical equations for a perfect pressureless fluid with density  $n$  and velocity potential  $\phi/m$ . The fluid equations consist of the continuity equation and the Bernoulli equation

$$\partial_t n = -\frac{1}{ma^2} \nabla \cdot (n \nabla \phi), \quad (8a)$$

$$\partial_t \phi = -\frac{1}{2a^2 m} (\nabla \phi)^2 - mV. \quad (8b)$$

By defining an irrotational velocity according to  $\mathbf{u} = \nabla \phi/m$  one can rewrite the fluid system in the following equivalent form

$$\partial_t n = -\frac{1}{a^2} \nabla \cdot (n \mathbf{u}), \quad (9a)$$

$$\partial_t \mathbf{u} = -\frac{1}{a^2} (\mathbf{u} \cdot \nabla) \mathbf{u} - \nabla V, \quad (9b)$$

$$\nabla \times \mathbf{u} = 0. \quad (9c)$$

### C. Coarse grained Vlasov equation

The coarse grained distribution function  $\bar{f}$  is obtained from  $f$  by convolution with a Gaussian of width  $\sigma_x$  and  $\sigma_p$  in  $\mathbf{x}$  and  $\mathbf{p}$  space, respectively. For convenience we will adopt the shorthand operator representation of the smoothing which can be easily obtained by switching to Fourier space

$$\begin{aligned} \bar{f}(\mathbf{x}, \mathbf{p}) &= \int \frac{d^3 x' d^3 p'}{(\pi \sigma_x \sigma_p)^3} \exp \left[ -\frac{(\mathbf{x} - \mathbf{x}')^2}{2\sigma_x^2} - \frac{(\mathbf{p} - \mathbf{p}')^2}{2\sigma_p^2} \right] f(\mathbf{x}', \mathbf{p}'), \\ \bar{f} &= \exp \left( \frac{\sigma_x^2}{2} \Delta_x + \frac{\sigma_p^2}{2} \Delta_p \right) f. \end{aligned} \quad (10)$$

The corresponding coarse grained Vlasov equation as given in [43] is easily obtained from the usual Vlasov equation (6) by applying the smoothing operator. We employ the following identity for the smoothing operator

$$\exp(\Delta)(AB) = [\exp(\Delta)A] \exp \left( 2 \overleftarrow{\nabla} \overrightarrow{\nabla} \right) [\exp(\Delta)B], \quad (11)$$

in order to express the coarse-graining of a product in terms of its coarse-grained factors. The result is the cosmological analogue to the evolution equation for coarse-grained classical mechanics as given in [28] for the special case where  $\sigma_x^2 = \sigma_p^2 = \hbar/2$

$$\partial_t \bar{f} = -\frac{\mathbf{p}}{a^2 m} \nabla_x \bar{f} - \frac{\sigma_p^2}{a^2 m} \nabla_x \nabla_p \bar{f} + m \nabla_x \bar{V} \exp(\sigma_x^2 \overleftarrow{\nabla}_x \overrightarrow{\nabla}_x) \nabla_p \bar{f}, \quad (12a)$$

$$= \exp \left( \frac{\sigma_x^2}{2} \Delta_x + \frac{\sigma_p^2}{2} \Delta_p \right) \left[ \frac{\mathbf{p}^2}{2a^2 m} + mV \right] \exp \left( \sigma_x^2 \overleftarrow{\nabla}_x \overrightarrow{\nabla}_x + \sigma_p^2 \overleftarrow{\nabla}_p \overrightarrow{\nabla}_p \right) \left( \overleftarrow{\nabla}_x \overrightarrow{\nabla}_p - \overleftarrow{\nabla}_p \overrightarrow{\nabla}_x \right) \bar{f}. \quad (12b)$$

Note that this result holds on a FRW background with cosmic time  $t$ , comoving  $\mathbf{x}$  and canonical conjugate 1-form  $\mathbf{p}$ , where

$\bar{V}$  fulfills Eq. (3b) where  $f$  is replaced by  $\bar{f}$ . If derivative oper-



ators like  $\nabla_x$  and  $\nabla_p$  carry left or right arrows over them, they specify that they only act on quantities on their left or right hand side, respectively. The notation of Eq. (12) is the same as used in [28].

At a first glance the coarse graining introduced in (10) might seem like an unfavorable artifact which complicates calculations on the one hand and erases relevant information on the other hand. However, one has to bear in mind that when sampling the distribution function numerically using a finite number of particles a coarse-graining is inevitable to provide a proper phase-space description [18]. This is of particular importance since solving the Vlasov-Poisson equation analytically is a formidable task and one typically has to resort to numerical simulations, for example N-body codes [2, 8–12]. The coarse grained phase space distribution function  $\bar{f}$  can therefore be seen as a theoretical N-body double.

## D. Husimi-Vlasov equation

### 1. Schrödinger Poisson system

The Schrödinger-Poisson system in a  $\Lambda$ CDM universe with scale factor  $a$  is given by

$$i\hbar\partial_t\psi = -\frac{\hbar^2}{2a^2m}\Delta\psi + mV(x)\psi, \quad (13a)$$

$$\Delta V = \frac{4\pi G\rho_0}{a}(|\psi|^2 - 1), \quad (13b)$$

see for instance [22]. Using the so-called Madelung representation for the wave function  $\psi(x) = \sqrt{n(x)}\exp(i\phi(x)/\hbar)$  one can obtain fluid-like equations of motion for the normalized density  $n^2$  and the velocity potential  $\phi$  directly from the Schrödinger equation [35]. By separating real and imaginary parts one obtains the continuity equation (8a), and an equation for  $\phi$  which is similar to the Bernoulli equation (8b) but contains an extra term proportional to  $\hbar^2$ , the so-called ‘quantum pressure’

$$\partial_t n = -\frac{1}{ma^2}\nabla \cdot (n\nabla\phi), \quad (14a)$$

$$\partial_t\phi = -\frac{1}{2a^2m}(\nabla\phi)^2 - mV + \frac{\hbar^2}{2a^2m}\frac{\Delta\sqrt{n}}{\sqrt{n}}, \quad (14b)$$

$$\Delta V = \frac{4\pi G\rho_0}{a}(n - 1). \quad (14c)$$

With the definition  $\mathbf{u} = \nabla\phi/m$ , the modified Bernoulli equation for  $\phi$  is then equivalent to a modified Euler equation with constraint  $\nabla \times \mathbf{u} = 0$ .

$$\partial_t n = -\frac{1}{a^2}\nabla_x \cdot (n\mathbf{u}), \quad (15a)$$

$$\partial_t \mathbf{u} = -\frac{1}{a^2}(\mathbf{u} \cdot \nabla)\mathbf{u} - \nabla V + \frac{\hbar^2}{2a^2m^2}\nabla \left( \frac{\Delta\sqrt{n}}{\sqrt{n}} \right). \quad (15b)$$

At this stage we want to emphasize again that the Schrödinger equation is considered here as a mere tool to model CDM dynamics. Therefore the value of  $\hbar$  has to be treated as a parameter which is not necessarily connected to the value of  $\hbar$  in the context of ordinary quantum mechanics, but rather must be adjusted to computational feasibility and the physical problem at hand [22]. Another important remark is in order. The Madelung representation Eqs. (14) is only equivalent to the Schrödinger system Eqs. (13) as long as  $n \neq 0$ . We will see later that during shell crossings interference in the wavefunction  $\psi$  will cause  $n = 0$  at isolated points in space and time. Once this happens the Madelung representation breaks down because  $\phi$  develops infinite spatial gradients and phase jumps, leading to infinite time derivatives. If one still prefers to stay in the fluid picture, one needs to solve instead for the momentum  $\mathbf{j} \equiv n\mathbf{u}$ , which is well behaved during these phase jumps. In App. (B) we investigate the Lagrangian formulation of the Madelung system, which suffers from the same problem.

### 2. Wigner quasi-probability distribution

Originally introduced to study quantum corrections to classical statistical mechanics, the Wigner quasi-probability distribution [44] allows to link the Schrödinger wavefunction  $\psi(x)$  to a function  $f(x, p)$  in phase space

$$f_W(x, p) = \int \frac{d^3\tilde{x}}{(\pi\hbar)^3} \exp\left[2\frac{i}{\hbar}\mathbf{p} \cdot \tilde{x}\right] \psi(x - \tilde{x})\psi^*(x + \tilde{x}). \quad (16)$$

$f_W$  is a quasi-probability distribution since it can become negative, for example for quantum states which have no classical analogue, see [45].

*Wigner Vlasov equation* The time evolution equation for  $f_W$  is obtained by using the Schrödinger equation and performing an integration by parts twice which yields

$$\partial_t f_W = -\frac{\mathbf{p}}{a^2m} \cdot \nabla_x f_W + \frac{i}{\hbar} \int \frac{d^3\tilde{x}}{(\pi\hbar)^3} \exp\left[2\frac{i}{\hbar}\mathbf{p} \cdot \tilde{x}\right] \times \quad (17)$$

$$\times m[V(x + \tilde{x}) - V(x - \tilde{x})] \psi(x - \tilde{x})\psi^*(x + \tilde{x}).$$

In order to obtain a factorization of the form  $V(x) \cdot f_W$  one has to perform a Taylor expansion of  $V(x - \tilde{x}) - V(x + \tilde{x})$  around  $x$  using  $\alpha \in \mathbb{N}_0^3$  as a multi-index

$$V(x + \tilde{x}) - V(x - \tilde{x}) = \sum_{|\alpha| \geq 1} \frac{1}{\alpha!} \partial_x^{(\alpha)} V(x) [\tilde{x}^\alpha - (-\tilde{x})^\alpha]. \quad (18)$$

Obviously the difference in parentheses vanishes if  $|\alpha|$  is even and gives  $2\tilde{x}^\alpha$  if  $|\alpha|$  is odd. Therefore this term can be rewritten as derivative  $-i\hbar\partial_p^{(\alpha)} \exp[2i\mathbf{p} \cdot \tilde{x}/\hbar]$ . Upon resummation one obtains the evolution equation for the Wigner function

$$\partial_t f_W = -\frac{\mathbf{p}}{a^2m} \cdot \nabla_x f_W + mV \frac{2}{\hbar} \sin\left(\frac{\hbar}{2} \overleftarrow{\nabla}_x \overrightarrow{\nabla}_p\right) f_W, \quad (19a)$$

$$= \left[ \frac{\mathbf{p}^2}{2a^2m} + mV \right] \frac{2}{\hbar} \sin\left(\frac{\hbar}{2} (\overleftarrow{\nabla}_x \overrightarrow{\nabla}_p - \overleftarrow{\nabla}_p \overrightarrow{\nabla}_x)\right) f_W, \quad (19b)$$

<sup>2</sup> The volume average is  $\langle n \rangle_{\text{vol}} = 1$ .

which coincides with the result given in [28] for the special case where  $a = 1$ . Note that on a FRW  $a(t)$  is the scale factor with  $t$  cosmic time,  $\mathbf{x}$  comoving,  $\mathbf{p}$  is the conjugate momentum 1-form and  $V$  fulfills Eq. (14c).

*Relation to  $f_d$*  The similarity between the equations (14) obtained from a Schrödinger wavefunction when decomposing it into modulus and phase  $\psi = \sqrt{n} \exp(i\phi/\hbar)$  and the fluid equations (32) can also be understood from the point of view of distribution functions. Transforming variables  $\tilde{\mathbf{x}} \rightarrow \hbar\tilde{\mathbf{x}}$  and adopting the short-hand notation  $g^\pm = g(\mathbf{x} \pm \hbar\tilde{\mathbf{x}})$  the Wigner function can be rewritten in the following form

$$f_W(\mathbf{x}, \mathbf{p}) = \int \frac{d^3\tilde{\mathbf{x}}}{\pi^3} \sqrt{n^+ n^-} \exp \left[ i \left( 2\mathbf{p} \cdot \tilde{\mathbf{x}} + \frac{\phi^- - \phi^+}{\hbar} \right) \right],$$

which allows to examine the formal limit  $\hbar \rightarrow 0$ . Taylor-expanding  $n^\pm$  and  $\phi^\pm$  to leading non-vanishing order in  $\hbar$  and evaluating the integral gives [22]

$$f_W(\mathbf{x}, \mathbf{p}) \xrightarrow{\hbar \rightarrow 0} n(\mathbf{x}) \delta(\mathbf{p} - \nabla\phi(\mathbf{x})) = f_d(\mathbf{x}, \mathbf{p}). \quad (20)$$

*Correspondence to Vlasov equation* At leading order, the Wigner Vlasov equation (19) differs from the Vlasov equation (6) only by a term proportional to  $\hbar^2$

$$\partial_t(f_W - f) \simeq \frac{\hbar^2}{24} \partial_{x_i} \partial_{x_j} \nabla_x V \partial_{p_i} \partial_{p_j} \nabla_p f_W + O(\hbar^4).$$

Therefore one might hope that they are in good agreement. However, as was shown exemplarily in [28], the correspondence between the time-evolution of the Wigner distribution  $f_W$  and the classical probability distribution function  $f$  is in general very poor by virtue of the violent oscillations of  $f_W$  on scales  $\hbar$ , related to the fact that  $f_W$  can become negative. In this context one has to bear in mind that the semiclassical limit  $\hbar \rightarrow 0$  is not meaningful in the sense that it does not drive the solution towards a classical one in a continuous way.

### 3. Coarse-grained Wigner distribution function

The so-called Husimi-Q [27] representation can be understood as a smoothing of the Wigner quasi-probability distribution by a Gaussian filter of width  $\sigma_x$  and  $\sigma_p$  in  $x$  and  $p$  space, respectively

$$\tilde{f}_W = \exp \left( \frac{\sigma_x^2}{2} \Delta_x + \frac{\sigma_p^2}{2} \Delta_p \right) f_W. \quad (21)$$

In contrast to the Wigner distribution itself the coarse grained version is a positive-semidefinite function if the filter is of appropriate size  $\sigma_x \sigma_p \geq \hbar/2$  for a semi-classical description, see [45]. Note that for the FRW case, the form of  $\tilde{f}_W$  remains unchanged provided  $\mathbf{x}$  is comoving and  $\mathbf{p}$  is the conjugate momentum 1-form.

*Husimi-Vlasov equation* The corresponding Husimi-Vlasov equation for the coarse grained  $f_W$  is then easily obtained by acting with the coarse-graining operators onto Eq. (19) employing again the product rule

$$\partial_t \tilde{f}_W = -\frac{\mathbf{p}}{a^2 m} \nabla_x \tilde{f}_W - \frac{\sigma_p^2}{a^2 m} \nabla_x \nabla_p \tilde{f}_W + m \bar{V} \exp(\sigma_x^2 \overleftarrow{\nabla}_x \overrightarrow{\nabla}_x) \frac{2}{\hbar} \sin \left( \frac{\hbar}{2} \overleftarrow{\nabla}_x \overrightarrow{\nabla}_p \right) \tilde{f}_W, \quad (22a)$$

$$= \exp \left( \frac{\sigma_x^2}{2} \Delta_x + \frac{\sigma_p^2}{2} \Delta_p \right) \left[ \frac{\mathbf{p}^2}{2a^2 m} + mV(\mathbf{x}) \right] \exp \left( \sigma_x^2 \overleftarrow{\nabla}_x \overrightarrow{\nabla}_x + \sigma_p^2 \overleftarrow{\nabla}_p \overrightarrow{\nabla}_p \right) \frac{2}{\hbar} \sin \left( \frac{\hbar}{2} (\overleftarrow{\nabla}_x \overrightarrow{\nabla}_p - \overleftarrow{\nabla}_p \overrightarrow{\nabla}_x) \right) \tilde{f}_W. \quad (22b)$$

This equation is the generalization of the result given in [28] allowing for cosmological backgrounds, arbitrary potentials and smoothing scales  $\sigma_x, \sigma_p$ . It is the resummation of the equation given upto second order in  $\sigma_x$  by [46] which was obtained by explicit calculation performed analogously to the one presented for  $f_W$ .

In [22] the Husimi representation was used instead, in which the wave function is represented in a (over-complete) basis of Gaussian wave packets

$$\psi_H(\mathbf{x}, \mathbf{p}) = (2\pi\hbar)^{-3/4} (2\pi\sigma_x^2)^{-3/2} \times \int d^3y \exp \left[ -\frac{(\mathbf{x} - \mathbf{y})^2}{4\sigma_x^2} - \frac{i}{\hbar} \mathbf{p} \cdot \left( \mathbf{y} - \frac{1}{2}\mathbf{x} \right) \right] \psi(\mathbf{y}), \quad (23a)$$

such that when going from  $\psi$  to  $\psi_H$  no information is sacrificed. Defining the Husimi distribution function to be

$$f_H = |\psi_H|^2, \quad (23b)$$

it is easy to check that  $f_H = \tilde{f}_W$  holds if  $\sigma_x \sigma_p = \hbar/2$ . This representation is very convenient numerically because  $f_H$  is manifestly real and positive. Also the integration is much simpler to evaluate than for  $f_W$ . The main advantage is that one does not need to sample the quite heavily oscillating  $f_W$  to construct  $\tilde{f}_W$ . Fig. 2 (1st panel) provides an impression of  $f_W$  for cold initial conditions. We also know that  $\sigma_x \sigma_p \geq \hbar/2$  ensures  $\tilde{f}_W \geq 0$ . Therefore the Husimi representation of  $\psi$  picks the optimal yet sufficient condition for a positive phase space distribution. Most notably, for cold dust-like initial conditions well within the linear regime we are free to choose even

$\sigma_x \sigma_p < \hbar/2$  without encountering any trouble, see Figs. 1 (1st panel) and 2 (2nd panel). It is important to realize that the dynamics at early times well before shell-crossing is not affected by the seemingly poor phase space resolution, see Fig. 1 (1st panel). We can realize this either by inspecting the Madelung representation (14) of the Schrödinger equation from which it is clear that for smooth dust-like initial conditions the quantum potential  $Q$  will be subdominant or simply by recalling that the mapping from  $\psi$  to  $f_H$  preserves information. However once  $f_H$  or  $\tilde{f}_W$  is used to calculate moments, information will be lost.

*Correspondence to coarse-grained Vlasov equation* Comparing the coarse grained Vlasov equation (12) and the Husimi-Vlasov equation (22) we find that they are equal at first order in  $\sigma_x^2$  and  $\sigma_p^2$

$$\partial_t (\tilde{f}_W - \tilde{f}) \simeq \frac{\hbar^2}{24} \partial_{x_i} \partial_{x_j} \nabla_x V \partial_{p_i} \partial_{p_j} \nabla_p \tilde{f}_W + O(\hbar^4, \hbar^2 \sigma_x^2). \quad (24)$$

The Husimi-Vlasov equation (22) is in good correspondence to the coarse grained Vlasov equation (12) if  $\sigma_x \sigma_p \gtrsim \hbar/2$ , which ensures the removal of the violent oscillations and therefore approximates the Vlasov equation well if  $\sigma_x \ll x_{\text{typ}}$  and  $\sigma_p \ll p_{\text{typ}}$ . Hereby we compared the two distribution functions which are obtained with the same coarse-graining parameters  $\sigma_x$  and  $\sigma_p$  in phase space. As described in [28], the coarse grained Wigner function  $\tilde{f}_W$  reveals a considerably better correspondence to the probability distribution function  $f$  in classical mechanics than the Wigner function  $f_W$  does.

#### 4. Appropriate choice of the smoothing scales

If  $x_{\text{typ}}$  and  $p_{\text{typ}}$  are the (minimal) scales of interest we have to ensure that

$$\sigma_x \ll x_{\text{typ}} \quad \text{and} \quad \sigma_p \ll p_{\text{typ}}. \quad (25)$$

Furthermore in general the maximal achievable resolution in phase space is limited by the value of  $\hbar$  such that  $\sigma_x$  and  $\sigma_p$  have to be chosen such that

$$\hbar/2 \lesssim \sigma_x \sigma_p, \quad (26)$$

see however Fig 1 for an exception. On a FRW background these bounds take the same form if distances are comoving and if  $u_{\text{typ}} = p_{\text{typ}}/m$  is the comoving (or canonical) momentum 1-form.

Translating these bounds into requirements for numerical simulations, grid time resolution, we refer the reader to [22].

### III. HIERARCHY OF MOMENTS

In practice one is usually interested in following the evolution of the spatial distribution instead of describing the fully-fledged phase-space dynamics encoded in the Vlasov equation. For this purpose, the relevant information can be extracted by taking moments of the distribution function with respect to momentum.

*Generating functional* The moments  $M^{(n)}$  of the phase space distribution function  $f(x, p)$  can be obtained from the generating functional  $G[J]$  by taking functional derivatives. In a similar way the cumulants can be determined from the moments. They provide a good way to understand the prominent dust-model which is the only known consistent truncation of the Vlasov hierarchy. The generating functional, moments and cumulants are given by

$$G[J] = \int d^3p \exp[i\mathbf{p} \cdot \mathbf{J}] f, \quad (27a)$$

$$M_{i_1 \dots i_n}^{(n)} := \int d^3p p_{i_1} \dots p_{i_n} f = (-i)^n \left. \frac{\partial^n G[J]}{\partial J_{i_1} \dots \partial J_{i_n}} \right|_{J=0}, \quad (27b)$$

$$C_{i_1 \dots i_n}^{(n)} := (-i)^n \left. \frac{\partial^n \ln G[J]}{\partial J_{i_1} \dots \partial J_{i_n}} \right|_{J=0}. \quad (27c)$$

*Vlasov hierarchy* The evolution equations for the moments  $M^{(n)}$  of the phase-space distribution  $f$  can be determined from the Vlasov equation (6a) by multiplying it with  $p_{i_1} \dots p_{i_n}$  and performing an integration over momentum

$$\partial_t M_{i_1 \dots i_n}^{(n)} = -\frac{1}{a^2 m} \nabla_j M_{i_1 \dots i_n j}^{(n+1)} - m \nabla_{(i_1} V \cdot M_{i_2 \dots i_n)}^{(n-1)}. \quad (28)$$

It turns out that a coupled Vlasov hierarchy for the moments emerges which means that in order to determine the time-evolution of the  $n$ -th moment the  $(n+1)$ -th moment is required. This closure problem for the hierarchy becomes more transparent when looking at the dynamical equation for the  $n$ -th cumulant  $C^{(n)}$ . The time evolution can be determined from the generating functional (27a) using the Vlasov equation (6a) and reads

$$\begin{aligned} \partial_t C_{i_1 \dots i_n}^{(n)} = & -\frac{1}{a^2 m} \left\{ \nabla_j C_{i_1 \dots i_n j}^{(n+1)} + \sum_{S \in \mathcal{P}(\{i_1, \dots, i_n\})} C_{l \notin S, j}^{(n+1-|S|)} \cdot \nabla_j C_{k \in S}^{(|S|)} \right\} \\ & - \delta_{n1} \cdot m \nabla_{i_1} V, \end{aligned} \quad (29)$$

where  $S$  runs through the power set  $\mathcal{P}$  of indices  $\{i_1, \dots, i_n\}$  and the last term containing the potential contributes only to the equation for the first cumulant  $C^{(1)}$  describing velocity. From this equation it becomes clear that one can set  $C^{(n \geq 2)} \equiv 0$  in a consistent manner since each summand in the evolution equation of  $C^{(2)}$  contains a factor of  $C^{(n \geq 2)}$ . In contrast, the time evolution of  $C^{(3)}$  depends also on summands containing solely  $C^{(2)}$  such that it cannot be trivially fulfilled when setting  $C^{(n \geq 3)} \equiv 0$ . A similar reasoning applies to all higher cumulants  $C^{(n \geq 3)}$  and demonstrates that there is no consistent truncation of the hierarchy of cumulants apart from the one at second order. These arguments are seconded by numerical evidence indicating that as soon as velocity dispersion encoded in  $C^{(2)}$  becomes relevant, even higher cumulants are sourced dynamically, see [20].

*Strategies for closing the hierarchy* In principle it would be desirable to adopt an ansatz for  $f$  which is the most general one. However, in this case it is impossible to find a closed form expression for the moments since one cannot perform the integration over momentum space. Therefore we have to resort to a special ansatz for the  $p$ -dependence of  $f$  which allows to compute moments upto arbitrary order analytically. In



the following we will compare three different ansätze for the distribution function  $f$ , the dust model  $f_d$ , the Wigner function  $f_W$  as well as the Husimi distribution function  $\tilde{f}_W$ .

### A. Hierarchy of moments of $f_d$

The generating functional for the dust model where  $f_d$  was inserted according to (7) is given by

$$G[\mathbf{J}] = n \exp[i \nabla \phi \cdot \mathbf{J}]. \quad (30)$$

The moments  $M_d^{(n)}$  and cumulants  $C_d^{(n)}$  are then given by

$$\begin{aligned} M_d^{(0)} &= n, & M_{d_i}^{(1)} &= n\phi_{,i}, & M_{d_{i_1 \dots i_n}}^{(n \geq 2)} &= n\phi_{,i_1} \dots \phi_{,i_n}, \quad (31a) \\ C_d^{(0)} &= \ln n, & C_{d_i}^{(1)} &= \phi_{,i}, & C_{d_{i_1 \dots i_n}}^{(n \geq 2)} &= 0. \quad (31b) \end{aligned}$$

Since the exponent of the generating functional is manifestly linear in  $\mathbf{J}$ , all cumulants of order higher than one vanish identically. This means that the dust model does not include effects like velocity dispersion which is encoded in the second cumulant  $C^{(2)}$  or vorticity since the velocity is determined from a potential  $\phi$ . Therefore for the dust ansatz  $f_d$  the Vlasov equation is equivalent to its first two equations of the hierarchy of moments, the pressureless fluid system consisting of the continuity and Euler equation, the first two moments of the Vlasov hierarchy Eq. (28)

$$\partial_t n = -\frac{1}{a^2 m} \nabla_k (n\phi_{,k}), \quad (32a)$$

$$\partial_t (n\phi_{,i}) = -\frac{1}{a^2 m} \nabla_j [n\phi_{,i}\phi_{,j}] - nm \nabla_i V. \quad (32b)$$

If  $n$  and  $\phi$  fulfill these equations then all evolution equations of the higher moments are automatically satisfied, for example Eqs. (32) imply that

$$\partial_t (n\phi_{,i}\phi_{,j}) = -\frac{1}{a^2 m} \nabla_k (n\phi_{,i}\phi_{,j}\phi_{,k}) - nm \nabla_i (V \cdot \nabla_j \phi). \quad (33)$$

Indices enclosed in round brackets imply symmetrization according to  $a_{(i}b_{j)} = a_i b_j + a_j b_i$ .

### B. Hierarchy of moments of $f_W$

For simplicity we first consider the Wigner distribution function  $f_W$  as a model for a general distribution function  $f$  described by the Vlasov equation. This case will serve as pedagogical demonstration how the closure of the hierarchy can be achieved by choosing a special ansatz for the distribution function. The generating functional can be computed by plugging the expression for  $f_W$  in terms of  $\psi = \sqrt{n} \exp(i\phi/\hbar)$  in (27a) and simplified by adopting again the short-hand notation  $g^\pm(\mathbf{x}') := g(\mathbf{x}' \pm \frac{\hbar}{2}\mathbf{J})$

$$G[\mathbf{J}] = \sqrt{n^+ n^-} \exp\left[\frac{i}{\hbar}(\phi^+ - \phi^-)\right]. \quad (34)$$

From this expression the calculation for the moments  $M^{(n)}$  is straightforward and yields

$$M^{(0)} = n, \quad M_i^{(1)} = n\phi_{,i}. \quad (35a)$$

As expected, even all higher moments  $M^{(n \geq 2)}$  of  $f_W$  are given in terms of the two scalar degrees of freedom  $n$  and  $\phi$  introduced as modulus and phase of the wavefunction  $\psi$ , respectively

$$M_{ij}^{(2)} = n \left[ \phi_{,i}\phi_{,j} + \frac{\hbar^2}{4} \left( \frac{n_{,i}n_{,j}}{n^2} - \frac{n_{,ij}}{n} \right) \right], \quad (35b)$$

$$M_{ijk}^{(3)} = n \left[ \phi_{,i}\phi_{,j}\phi_{,k} + \frac{\hbar^2}{4} \left( \left( \frac{n_{,i}n_{,j}}{n^2} - \frac{n_{,ij}}{n} \right) \phi_{,k} - \phi_{,ijk} \right) \right], \quad (35c)$$

$$C_{ij}^{(2)} = \frac{\hbar^2}{4} \left( \frac{n_{,i}n_{,j}}{n^2} - \frac{n_{,ij}}{n} \right) =: \sigma_{ij}, \quad C_{ijk}^{(3)} = -\frac{\hbar^2}{4} \phi_{,ijk}. \quad (35d)$$

To those terms which are marked by ‘+ cyc. perm.’ cyclic permutations of the indices have to be added. As we will explain in the following, this special form of the higher moments and cumulants amounts to having closed the infinite Wigner-Vlasov hierarchy for the moments of  $f_W$  without truncating it. To demonstrate this we take moments of the Wigner-Vlasov equation (19) where we consider corrections to the Vlasov equation up to arbitrary order in  $\hbar^2$ . The  $\hbar$ -terms constitute correction terms to the Vlasov hierarchy (28) which become relevant for  $M^{(n \geq 3)}$  but do not contribute to  $M^{(n \leq 2)}$  since they have at least three derivatives with respect to momentum which cancel all lower moments than the third. Therefore the first three evolution equations are completely analogous to the ones obtained for the dust model. By plugging in the expression for  $M^{(2)}$  we obtain a closed system of differential equations for  $n$  and  $\phi_{,i}$ .

$$\partial_t n = -\frac{1}{a^2 m} \nabla_k (n\phi_{,k}), \quad (36a)$$

$$\partial_t (n\phi_{,i}) = -\frac{1}{a^2 m} \nabla_j \left[ n\phi_{,i}\phi_{,j} + \frac{\hbar^2}{4} \left( \frac{n_{,i}n_{,j}}{n} - n_{,ij} \right) \right] - nm \nabla_i V. \quad (36b)$$

We see that Eqs. (36) determining time evolution of the first two moments of  $f_W$  are identical to the fluid-like equations obtained directly from the Schrödinger equation (14). This can be verified easily by plugging (36a) into (36b) and using that the difference in the ‘quantum velocity dispersion’ term arising from (41c) and (14b) is only apparent since

$$\frac{\hbar^2}{4} \nabla_j \left( \frac{n_{,i}n_{,j}}{n} - n_{,ij} \right) = -\frac{\hbar^2}{2} n \nabla_i \left( \frac{\Delta \sqrt{n}}{\sqrt{n}} \right). \quad (37)$$

Note that a proper pressure term in the Euler equation would have the form  $\nabla p$  with some  $p$  and not the form  $n \nabla Q$ . Rather the left hand side of (36b) suggests that this term constitutes a ‘quantum velocity dispersion’, since it is of the form  $\nabla_i (n \sigma_{ij})$ . Equivalently, one can interpret the  $\hbar$  term as a correction to the Newtonian potential  $V \rightarrow V + Q$  with

$$Q = -\frac{\hbar^2}{(2a^2 m^2)} \frac{\Delta \sqrt{n}}{\sqrt{n}}. \quad (38)$$

The evolution equation for the second moment  $M^{(2)}$  involves the third moment  $M^{(3)}$  and is given by

$$\partial_t M_{ij}^{(2)} = -\frac{1}{a^2 m} \nabla_k M_{ijk}^{(3)} - nm \nabla_{(i} V \cdot \nabla_{j)} \phi. \quad (39)$$

For the Wigner function  $f_W$  all moments  $M^{(n)}$  can be expressed entirely in terms of the density  $n$  and conjugate velocity  $\nabla \phi$ . This ansatz closes the hierarchy since Eq. (39) is automatically fulfilled when  $M^{(2)}$  and  $M^{(3)}$ , taken from (35b) and (35c) respectively, are expressed in terms of  $\bar{n}$  and  $\bar{v}$  which are to be determined from the coarse grained fluid equations (36). The same is true for all higher moments.

### C. Hierarchy of moments of $\bar{f}_W$

#### 1. Moments upto third order

We have to resort to a special ansatz for the  $p$ -dependence of  $f$  which allows to compute moments upto arbitrary order analytically. The coarse grained Wigner distribution function  $\bar{f}_W$  provides us with such an ansatz. Furthermore it is well-suited to model a general distribution function  $f$  fulfilling the Vlasov equation as was demonstrated in [22]. By plugging in the expression for  $\bar{f}_W$  in terms of  $\psi = \sqrt{n} \exp(i\phi/\hbar)$  we can rewrite the generating functional to get

$$G[J] = \exp \left[ \frac{\sigma_x^2}{2} \Delta - \frac{\sigma_p^2}{2} J^2 \right] \sqrt{n^+ n^-} \exp \left[ \frac{i}{\hbar} (\phi^+ - \phi^-) \right]. \quad (40)$$

From this expression the calculation for the moments  $\bar{M}^{(n)}$  is straightforward and yields

$$\bar{M}^{(0)} =: \bar{n} = \exp \left( \frac{\sigma_x^2}{2} \Delta \right) n, \quad (41a)$$

$$\bar{M}_i^{(1)} =: m \bar{n} \bar{u}_i = \exp \left( \frac{\sigma_x^2}{2} \Delta \right) (n \phi_{,i}). \quad (41b)$$

The corresponding velocity  $\bar{u} = a\bar{v}$  is a mass-weighted one which is obtained by smoothing the momentum field and then dividing by the smoothed density field. This is precisely the definition commonly used in the effective field theory of large scale structure, compare [47, 48]. From a physical point of view  $\bar{u}$  describes the center-of-mass velocity of the collection of particles inside a coarsening cell of diameter  $\sigma_x$  around  $x$ . As expected, even all higher moments  $\bar{M}^{(n \geq 2)}$  of  $\bar{f}_W$  are given in terms of the two scalar degrees of freedom  $n$  and  $\phi$  introduced as modulus and phase of the wavefunction  $\psi$ , respectively

$$\bar{M}_{ij}^{(2)} = \exp \left( \frac{\sigma_x^2}{2} \Delta \right) \left\{ n \left[ \phi_{,i} \phi_{,j} + \sigma_p^2 \delta_{ij} + \sigma_{ij} \right] \right\}, \quad (41c)$$

$$\bar{M}_{ijk}^{(3)} = \exp \left( \frac{\sigma_x^2}{2} \Delta \right) \left\{ n \left[ \phi_{,i} \phi_{,j} \phi_{,k} + \left( \sigma_p^2 \delta_{ij} + \sigma_{ij} \right) \phi_{,k} - \frac{\hbar^2}{4} \phi_{,ijk} \right] \right\}. \quad (41d)$$

The corresponding cumulants can be calculate from the previous results using

$$C_{ij}^{(2)} = \frac{\bar{M}_{ij}^{(2)}}{\bar{M}^{(0)}} - \frac{\bar{M}_i^{(1)} \bar{M}_j^{(1)}}{[\bar{M}^{(0)}]^2} \quad (41e)$$

$$= \sigma_p^2 \delta_{ij} + \frac{\overline{n \sigma_{ij}}}{\bar{n}} + \frac{\overline{n \phi_{,i} \phi_{,j}}}{\bar{n}} - \frac{\overline{n \phi_{,i}} \overline{n \phi_{,j}}}{\bar{n}^2}, \quad (41f)$$

$$C_{ijk}^{(3)} = \frac{\bar{M}_{ijk}^{(3)}}{\bar{M}^{(0)}} - \frac{\bar{M}_{ij}^{(2)} \bar{M}_k^{(1)}}{[\bar{M}^{(0)}]^2} + 2 \frac{\bar{M}_i^{(1)} \bar{M}_j^{(1)} \bar{M}_k^{(1)}}{[\bar{M}^{(0)}]^3} \quad (41g)$$

$$= \frac{\bar{M}_{ijk}^{(3)}}{\bar{M}^{(0)}} - \overset{+ \text{cyc. perm.}}{\bar{C}_{ij}^{(2)} \bar{C}_k^{(1)}} - \bar{C}_i^{(1)} \bar{C}_j^{(1)} \bar{C}_k^{(1)}. \quad (41h)$$

As we will explain in the following this allows to close the infinite hierarchy for the moments of  $\bar{f}_W$  arising from the Husimi-Vlasov Eq. (22) without setting any of the cumulants to zero. Instead, all higher moments are determined self-consistently from the lower ones which are dynamical and represent the coarse-grained density  $\bar{n}$  and velocity  $\bar{u}$ , respectively. This distinguishes our formalism fundamentally from phenomenological models which attempt to close the hierarchy by postulating an ansatz for the second cumulant, called stress tensor  $\sigma_{ij}$ , but simultaneously setting all higher cumulants to zero. For example, the ansatz for the velocity dispersion of a cosmological imperfect fluid is given by  $n \sigma_{ij} = p \delta_{ij} + \eta (\nabla_i u_j \nabla_j u_i - \frac{2}{3} \delta_{ij} \nabla \cdot u) + \zeta \delta_{ij} \nabla \cdot u$  where  $p$  denotes the pressure and  $\eta$  and  $\zeta$  are shear and bulk viscosity coefficients respectively. The underlying approximation  $\sigma_{ij} \approx 0$  is valid during the first stages of gravitational instability when structures are well described by a single coherent flow (single stream) since they did not yet collapse and virialise. However, as soon as multiple streams become relevant after shell-crossings, velocity dispersion and vorticity are generated dynamically and at once all higher moments become relevant too [20]. Thus, the hierarchy of cumulants of CDM dynamics cannot be truncated after shell crossing has occurred.

In the subsequent calculation it will be necessary to reexpress all higher moments entirely in terms of  $\bar{M}^{(0)} \propto \bar{n}$  and  $\bar{M}^{(1)} \propto \bar{n} \bar{v}_i$ . For this purpose we introduce the  $D$ -symbol which allows us to express the coarse-graining of any product or quotient entirely in terms of its coarse-grained constituents, for example

$$\exp \left[ \frac{1}{2} \sigma^2 \Delta \right] (n \phi_{,i} \phi_{,j}) = \exp \left[ \frac{1}{2} \sigma^2 (\Delta - D) \right] \left( \frac{(\bar{n} \bar{v}_i)(\bar{n} \bar{v}_j)}{\bar{n}} \right). \quad (42)$$

#### 2. Properties of the $D$ -symbol

$D$  fulfills the Leibniz product rule of a first derivative operator when acting on compositions of

$$A, B, C \in \{\bar{n}, \bar{n} \bar{v}_i\}$$

or derivatives thereof, but when acting on a single function it acts as the Laplacian.

$$D(A) = \Delta A, \quad D(g(A)) = \partial_A g(A) DA = \partial_A g(A) \Delta A, \quad (43a)$$

$$D(AB) = (DA)B + A(DB) = (\Delta A)B + A(\Delta B). \quad (43b)$$

Applying the definition of the  $D$ -symbol one can derive the following expressions for the evaluation of  $D^n$

$$D^n \left( \frac{AB}{C} \right) = \sum_{k=0}^n \binom{n}{k} \sum_{l=0}^{n-k} \binom{n-k}{l} \Delta^l A \cdot \Delta^{n-k-l} B \cdot D^k \left( \frac{1}{C} \right), \quad (44a)$$

$$D^k \left( \frac{1}{C} \right) = \sum_{r=0}^k \frac{(-1)^r r!}{C^{r+1}} B_{k,r} (\Delta C, \Delta^2 C, \dots, \Delta^{k-r+1} C), \quad (44b)$$

where  $B_{k,r}$  are the Bell polynomials. Furthermore we have that

$$\frac{1}{\exp(\sigma_x^2 \Delta) C} = \exp(\sigma_x^2 D) \left( \frac{1}{C} \right). \quad (44c)$$

### 3. Evolution equations for the moments of $\tilde{f}_W$

We take moments of the Husimi-Vlasov equation where we consider corrections to the Vlasov equation up to arbitrary order in  $\sigma_x^2$ ,  $\sigma_p^2$  and  $\hbar^2$ . Eq. (22) can be employed to obtain evolution equations for the first two moments  $\bar{n} = M^{(0)}$  and  $\bar{u}_i = a\bar{v}_i = M_i^{(1)}/(m\bar{n})$  which correspond to density and mass-weighted velocity, respectively. The velocity  $\bar{u}_i$  which follows from a coarse-grained distribution function  $\tilde{f}$  is automatically a mass-weighted one computed according to  $m\bar{u}_i = \bar{n}\phi_{,i}/\bar{n} \neq \bar{\phi}_{,i}$  and does not coincide with the volume-weighted velocity  $\bar{\phi}_{,i}$ . In particular, the volume-weighted velocity is automatically curl-free whereas the mass-weighted velocity will have vorticity in general.

By plugging in the expression for  $M^{(2)}$  and rewriting it according to (42) we obtain a closed system of differential equations for  $\bar{n}$  and  $\bar{v}_i$ .

$$\partial_t \bar{n} = -\frac{1}{a} \nabla_k (\bar{n} \bar{u}_k) = -\nabla_k (\bar{n} \bar{v}_k), \quad (45a)$$

$$\begin{aligned} \partial_t (\bar{n} \bar{u}_i) &= -\frac{1}{a^2 m^2} \nabla_j \bar{M}_{ij}^{(2)} - \nabla_i \bar{V} \exp \left( \sigma_x^2 \overleftarrow{\nabla}_x \overrightarrow{\nabla}_x \right) \bar{n} + \frac{\sigma_p^2}{a^2 m^2} \nabla_i \bar{n}, \\ (\mathcal{H} + \partial_t) (\bar{n} \bar{v}^i) &= \exp \left[ \frac{\sigma_x^2}{2} (\Delta - D) \right] \left\{ -\nabla_j \left[ \frac{(\bar{n} \bar{v}^j) (\bar{n} \bar{v}^i)}{\bar{n}} \right] - \bar{n} \nabla_i \bar{V} \right. \\ &\quad \left. + \frac{\hbar^2}{2m^2 a^2} \bar{n} \nabla_i \left( \frac{\Delta \sqrt{\bar{n}}}{\sqrt{\bar{n}}} \right) \right\}. \end{aligned} \quad (45b)$$

These equations are supplemented by the constraint that there exists a scalar function  $\bar{\phi}$  such that

$$m\bar{n} \bar{u}_i = \bar{n} \exp \left( \sigma_x^2 \overleftarrow{\nabla}_x \overrightarrow{\nabla}_x \right) \nabla_i \bar{\phi}. \quad (45c)$$

The last constraint equation is the analogue of the curl-free constraint Eq. (9c). It enforces a very particular non-zero vorticity for  $\bar{\mathbf{u}}$ . The evolution equation for the second moment

$M^{(2)}$  involves the third moment  $M^{(3)}$  and is given by

$$\begin{aligned} \partial_t \bar{M}_{ij}^{(2)} &= -\frac{1}{a^2 m} \nabla_k \bar{M}_{ijk}^{(3)} - m \nabla_{(i} \bar{V} \exp \left( \sigma_x^2 \overleftarrow{\nabla}_x \overrightarrow{\nabla}_x \right) (\bar{n} \bar{u}_{j)}) \\ &\quad + \frac{\sigma_p^2}{a^2} (\bar{n} \bar{u}_{(i,j)}). \end{aligned} \quad (46)$$

For the Husimi distribution function  $\tilde{f}_W$  all moments  $M^{(n)}$  can be expressed entirely in terms of the density  $\bar{n}$  and peculiar velocity  $\bar{\mathbf{v}}$ . This ansatz closes the  $\tilde{f}_W$  hierarchy since all higher moment equations are automatically fulfilled when  $M^{(n)}$  is calculated from (40), expressed in terms of  $\bar{n}$  and  $\bar{\mathbf{v}}$  which are to be determined from the coarse grained fluid equations (45). In appendix A we show by explicit computation that Eq. (33) is automatically satisfied when  $M^{(2)}$  and  $M^{(3)}$  are taken from (41c) and (41d) respectively.

Alternatively and for practical applications, instead of solving the coarse grained fluid equations (45) for  $\bar{n}$  and  $\bar{\mathbf{v}}$  one can simply solve the SPE (13) for  $n$  and  $\phi$  and construct the cumulants of interest according to (41). Both procedures automatically and self-consistently include multi-streaming effects. Note that Eqs. (45) are naturally written in terms of the macroscopic momentum  $\bar{\mathbf{j}} \equiv \bar{n} \bar{\mathbf{u}}$ , which is just the coarse grained quantum momentum, which therefore is free from phase jump pathologies, see Sec. IID 1.

### D. Comparison between the models

If we compare the fluid equations obtained via the Husimi approach Eqs. (45) with the one obtained directly from the Madelung representation Eqs. (14) of the underlying Schrödinger-Vlasov system we see that our special ansatz for the distribution function  $f = \tilde{f}_W$  amounts to considering a spatially coarse grained Schrödinger-Vlasov system. However, we have to bear in mind that this is not equivalent with a direct coarse graining of  $n$  and  $\phi_{,i}$  since the mass-weighted velocity is  $m\bar{u}_i = \bar{n}\phi_{,i}/\bar{n} \neq \bar{\phi}_{,i}$  is not the same as the volume-weighted velocity  $\bar{\phi}_{,i}$ . It is nontrivial that although  $\tilde{f}_W$  is coarse-grained with respect to space and momentum, the Schrödinger equation (14) and the first moment equations (45) of  $\tilde{f}_W$  are related only by spatial coarse graining. This is due to our special ansatz which causes  $\sigma_p$  to effectively drop out of (45). Note however that for instance the velocity dispersion  $\bar{C}_{ij}^{(2)}$  does depend on  $\sigma_p$  as well as on  $\sigma_x$  and  $\hbar$ , see Eq. (41c).

When neglecting the  $\hbar$  corrections which constitute a ‘quantum velocity dispersion’ term in the Bernoulli equation in (45b) we obtain the same evolution equations for the coarse grained fields  $\bar{n}$  and  $\bar{\mathbf{u}}$  as given in [17, 18]. The coarse graining contributions in (45b) act as adhesion-like terms and regularize shell-crossing singularities which usually appear as 1-dimensional caustics within the dust model. This was shown exemplarily in [17] where the smoothing operator  $\exp \left[ \frac{1}{2} \sigma_x^2 \Delta \right]$  was expanded upto first order in a so-called large-scale expansion. Furthermore, numerical examples show that the  $\hbar$ -term regularizes shell-crossing caustics already on the microscopic level, see [24, 28] and the next section. This is desirable since it allows to invert the smoothing operator which is needed to

derive closed-form equations for the macroscopic variables as done in (42).

Therefore the Schrödinger method may be viewed as improved dust model with built-in infinity regularisation (quantum velocity dispersion proportional to  $\hbar^2$ ) as well as built-in eraser of regularization artifacts (spatial coarse-graining with  $\sigma_x$ ). Nearly cold initial conditions can be implemented by choosing

$$\psi_{\text{ini}}(x) = \sqrt{n_d(a_{\text{ini}}, x)} \exp[i\phi_d(a_{\text{ini}}, x)/\hbar], \quad (47)$$

at some early time where shell crossings haven't occurred yet. Although we have our focus on cold dark matter, let us remark that ScM also opens up the possibility to study warm initial conditions.

#### IV. NUMERICAL EXAMPLE

We study the standard toy example of sine wave collapse, whose exact solution up to shell crossing is given by the (in this case exact) Zel'dovich approximation [21] and therefore has a long tradition in testing techniques of LSS calculations [49]. Of particular relevance to our work is [24] where the collapse of a wave function fulfilling the Schrödinger poisson equation and modifications to it were studied and compared to the exact Zel'dovich solution.

##### A. Initial conditions

As reviewed in App. B, the Zel'dovich approximation in the 1D (or plane parallel or pancake) collapse is the exact solution to the hydrodynamic equations Eqs. (9). We choose as initial linear density contrast

$$\delta_{\text{lin}}(a, q) = D(a) \cos\left(\frac{\pi q}{L}\right), \quad (48)$$

which guarantees collapse at  $a = 1$ , because according to Eq. (B4) the nonlinear density for dust is given by  $n_d(a, q) = [1 - \delta_{\text{lin}}(a, q)]^{-1}$  choosing  $D(1) = 1$ . The displacement field  $\Psi$  describes the trajectories  $x(q) = q + \Psi(a, q)$  of fluid elements and is given by

$$\Psi_d(a, q) = -D(a)L/\pi \sin(\pi q/L), \quad (49)$$

which can be used to express the velocity  $\partial_x \phi_d = u_d(q) = a^3 H(a) \partial_a \Psi_d(a, q)$  and density  $n_d$  in terms of  $x$ . We choose an Einstein-de Sitter universe,  $H^2 = 8\pi G/3 \rho_0 a^{-3}$  with  $H(a = 1) = 70 \text{ km s}^{-1} \text{ Mpc}^{-1}$  and we pick  $L = 10 \text{ Mpc}$ .

We start to solve the Schrödinger equation at  $a_{\text{ini}} = 0.01$  and choose as initial wave function Eq. (47). We verified that during the linear stage of collapse, the phase  $\phi$  and amplitude  $n$  of the wave function, agree with their dust analogues  $\phi_d$  and  $n_d$  if  $\tilde{\hbar} \equiv \hbar/m < 5 \times 10^{-3} \text{ Mpc } c$ , where  $c$  is the speed of light, which we set to  $c = 1$  in the following. This agrees

with findings of [24]. In the remaining section we will mostly show results for  $\tilde{\hbar} = 2 \times 10^{-5} \text{ Mpc}$ . Only for the study of relaxation ( $a = 30.0$  in the following plots) as well as the Bohmian trajectories – the integral lines of  $\partial_x \phi$  – in App. B we choose the larger value  $\tilde{\hbar} = 10^{-4} \text{ Mpc}$ . Note that the mass  $m$  can be absorbed in  $\phi$  and  $\phi_d$  and thereby  $m$  disappears from the Schrödinger and fluid equations, respectively. The Wigner and coarse grained Wigner functions are depicted in Fig. 2.

It turns out that in single streaming regions one can choose  $\sigma_x \sigma_p \ll \hbar$  while still ensuring  $\tilde{f}_W \geq 0$ , see Fig. 2. Comparing to the top panel of Fig. 1, it becomes clear that  $\tilde{f}_W$  can achieve a much higher resolution than  $f_H$  in  $u$ -direction. It exemplifies that the initial conditions are well modelled by the SPE and that the large width of  $f_H$  in the initial conditions shown in Fig. 1 does not imply that the dynamics is poorly resolved. In contrast, it only means that if we want to use the more convenient  $f_H$  we sacrifice available information once we calculate moments and cumulants. Another possibility to circumvent the oscillatory behaviour of the Wigner function is to use a mixed state corresponding to  $N$  gravitating wave functions rather than a single one. This was the method of choice in [40]. It turns out that if  $N$  is large enough, the Wigner function becomes well behaved even without any smoothing. Since our goal is to develop analytical tools on the basis of the ScM, it seems to be more prospective to consider a single wave function and adopt the Husimi representation.

##### B. Time evolution of $\psi$ , $f_H$ and moments

We numerically evolve the initial wave function  $\psi$  Eqs. (47, 48) describing a nearly cold and linear CDM overdensity using the SPE. Within the linear regime the phase  $\phi_{\text{ini}}$  and amplitude  $n$  are basically indistinguishable from  $\phi_d$  and  $n_d$ , however once shell crossing is approached they start to deviate. The occurrence of phase jumps is the most dramatical difference.

In Fig. 4 we show the phase closely before and after the time of first phase jump  $a_\phi$ , shortly after the time  $a = 1$ , where dust would run into the shell-crossing singularity. Shortly before (*full*) and after (*dotted*)  $a_\phi$ ,  $\phi$  develops very steep gradients (diverging at the time of phase jump). For the wave function  $\psi$  this causes no problem since the amplitude  $\sqrt{n}$  vanishes when the step becomes infinitely sharp and allows the phase to “reconnect” (*upper panel*) afterwards.

For the Madelung representation this causes a problem: at the moment of phase jump, not only  $\nabla \phi$  but also  $\phi$  diverge on a whole spatial interval (*lower panel*). At the time  $a_\phi$  and point  $x_\phi$  where the phase develops the sharp step we have  $\sqrt{n} = 0$ . Therefore it makes sense to ask what is

$$\langle x^2 \rangle = \frac{\int_{-x_\phi}^{x_\phi} |\psi|^2 x^2 dx}{\int_{-x_\phi}^{x_\phi} |\psi|^2 dx}, \quad (50)$$

$$\langle p^2 \rangle = -\hbar^2 \frac{\int_{-x_\phi}^{x_\phi} \psi^* \Delta \psi dx}{\int_{-x_\phi}^{x_\phi} |\psi|^2 dx}, \quad (51)$$

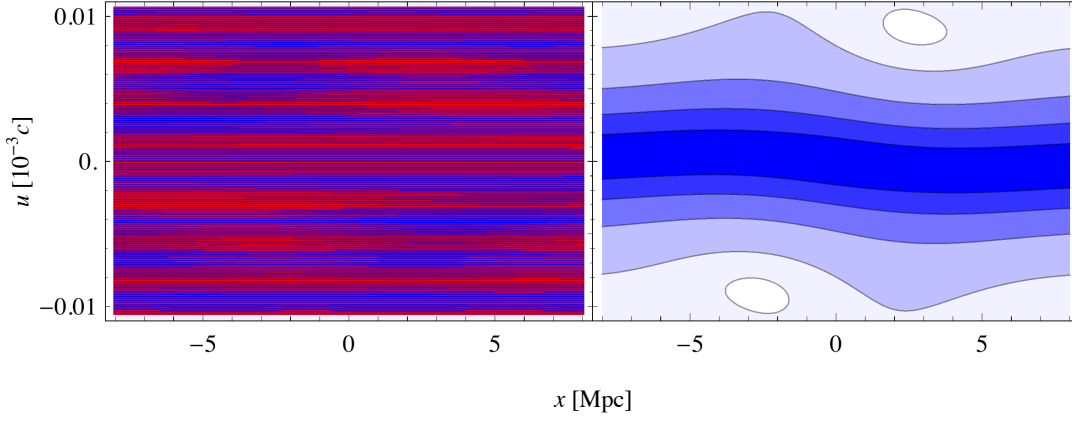


FIG. 2. Comparison between  $f_W$  and  $\bar{f}_W$  at the initial time  $a_{\text{ini}} = 0.01$ . The left panel shows the strongly oscillating  $f_W$  (red is negative, blue is positive), the right panel is its smoothed version  $\bar{f}_W$  (with the same coloring as in Fig 1). We choose the minimal values of  $\sigma_x$  and  $\sigma_p$  such that  $\bar{f}_W \geq 0$ , which turned out to be  $\sigma_x \sigma_p = 0.03\hbar$

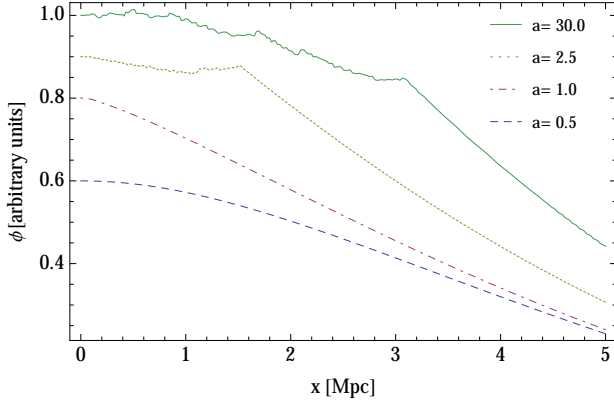


FIG. 3. The phase  $\phi$  of the wave function at times  $a = 0.5, 1.0, 2.5, 30.0$  from bottom to top. The wiggly behaviour is characteristic for multi streaming regions. All those wiggles originate from phase jumps.

the variance of position and momentum. Doing the numerical integrals it turns out that  $\langle x^2 \rangle \langle u^2 \rangle \simeq (\hbar/(2m))^2$ , with  $\hbar/(2m) = 10^{-5}$  specified for our simulation. The physical interpretation of this result is that the wave function collapsed to its densest possible state given the initial conditions: a minimum uncertainty wave packet forms in between  $[-x_\phi, x_\phi]$  at the time  $a_\phi$ , which expands consequently. This bounce looks like shell crossing when coarse grained over, see App. B. The result also suggests optimal values for the coarse graining parameters  $\sigma_u^2 = \langle u^2 \rangle$ ,  $\sigma_x^2 = \langle x^2 \rangle$  of the 1D collapse.

We therefore conclude that shell crossing infinities appearing in  $n_d$  are now treated for infinities in  $\nabla\phi$ , which fortunately do not cause infinities in  $\psi$  because  $n$  vanishes at those instances and  $\psi$  remains smooth.

The wiggly form of the phase corresponds to large  $\nabla\phi$ , which are visible as the strongly oscillating green dotted lines in the right panel of Fig. 7. Because of many phase jumps

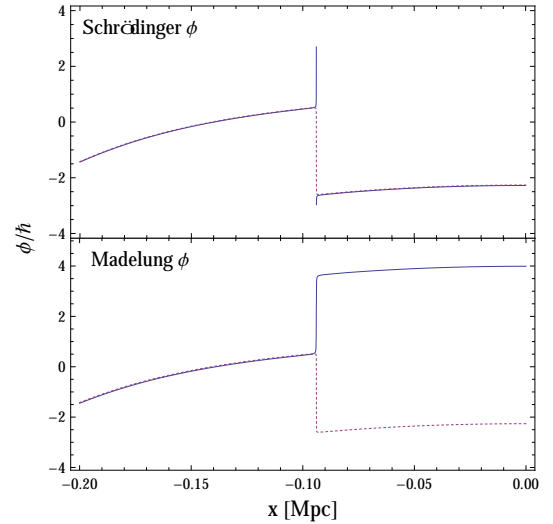


FIG. 4. The first phase jump about  $\Delta\phi = 2\pi$  occurred around  $a_\phi \simeq 1.07$ .

the  $n$  shows strong spatial oscillations Fig. 7, left. These oscillations are however irrelevant for the physical quantities of interest: the moments and cumulants of  $f_H$ . We also show the first 4 cumulants in Fig. 7 that are smooth and physically meaningful.

It is also interesting to note that  $\bar{C}^{(2)}$ , Eq. (41f), can be decomposed into a purely spatial average induced velocity dispersion, a smoothed but microscopic velocity dispersion and a constant part. Most notably, the first two contributions are equally large and show oscillations over time but add up to a smooth sum, see Fig. (5).

Finally let us consider the full phase space dynamics in Fig. (1), which contains information about all cumulants. The most interesting features we have already emphasized are the regularity at shell crossing, the formation of multi-stream regions and possibility to follow the dynamics until virialisa-



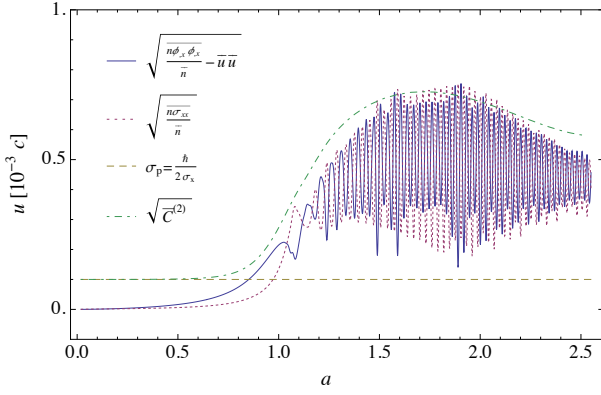


FIG. 5. Comparison between the different parts of the second cumulant at  $x = 0$ .

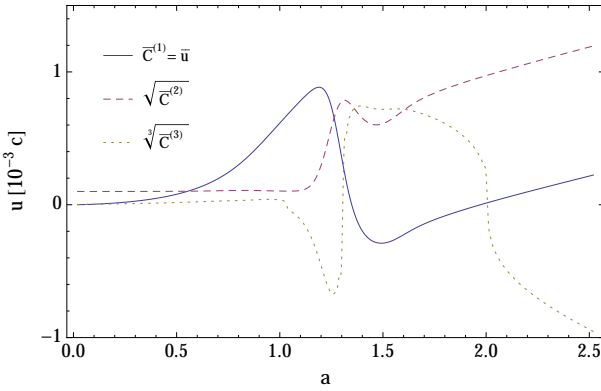


FIG. 6. Comparison between the first three cumulants at the position  $x = -0.5$  Mpc. They are all equally important after shell crossing: the hierarchy cannot be truncated.

tion. Notice that during the transition from over to under-density regions in phase space,  $\bar{C}^{(3)}$  changes sign, while  $\bar{C}^{(2)}$  within multi-stream regions remains always positive and  $\bar{C}^{(1)}$  basically vanishes.

We checked the (macroscopic) tensor virial theorem [50], that follows from the Euler-type equation (45b) and a steady state assumption, that within the virialised object  $\bar{u} = 0$ ,

$$2\bar{K}_{xx} \equiv \frac{1}{a^2} \int_{-x_{\text{vir}}}^{x_{\text{vir}}} dx (\bar{M}_{xx}^2 - \sigma_p^2 \bar{n}) = \int_{-x_{\text{vir}}}^{x_{\text{vir}}} dx x \exp[\frac{1}{2}\sigma_x^2 \Delta] (n(x) \partial_x V(x)) \equiv -\bar{W}_{xx} \quad (52)$$

is approximately satisfied for  $x_{\text{vir}} \approx 1.5$  for  $2.5 < a < 30$ . The  $\sigma_p$ -term is completely negligible. Looking at the right panel of Fig. 7 we see that below  $x_{\text{vir}}$  the macroscopic velocity  $\bar{u}$  is basically zero for  $a = 2.5$  and  $a = 30.0$ , looking at the left panel we see that the macroscopic density peaks around  $x_{\text{vir}}$  and drops off afterwards. For  $a = 30.0$  there is a second peak, which looking again at  $\bar{u}$  on the right, is still falling in.

We would like to refer the reader to App. B and Figs. 8, 9 for a better understanding of how “shell crossing without shell crossing” is possible in the ScM.

## V. PROSPECTS

For analysing, understanding as well as estimating covariances of observations of LSS one is interested in  $n$ -point correlation functions of the phase space density. In the ScM these correlation functions are simply related to the  $2n$ -point correlation functions of the complex scalar  $\psi$

$$\langle f(t, \mathbf{r}_1, \mathbf{p}_1) \dots f(t, \mathbf{r}_n, \mathbf{p}_n) \rangle = \int d^3x_1 \dots d^3x_{2n} K(\mathbf{x}_i, \mathbf{r}_i, \mathbf{p}_i) \langle \psi(t, \mathbf{x}_1) \dots \psi(t, \mathbf{x}_{2n}) \rangle, \quad (53)$$

where  $K$  is the product of  $n$  Husimi kernels Eq. (23). This allows the construction of  $n$ -point redshift space matter and halo correlation functions upon integration over

$$\Pi_i \delta_D(\mathbf{s}_i - \mathbf{r}_i - \mathbf{p}_i \cdot \hat{\mathbf{z}} / (a^2 m H) \hat{\mathbf{z}}) d^3p_i d^3r_i,$$

where  $\hat{\mathbf{z}}$  points along the line of sight. As a first step one can study the redshift space 2-point correlation in the case where  $\hbar = 0$ , keeping only  $\sigma_x$  and  $\sigma_p$  [51]. This approach is motivated by the observation that keeping only  $\sigma_x$ , results in a resummation in the large scale parameter of the macroscopic model suggested in [17, 18].

Ultimately we would like to keep  $\hbar$ , since from our numerical study it is clear that the quantum pressure plays a crucial role not only in shell crossing regularisation but also within the cumulants, see Fig. 5 left panel. Therefore we need a method to calculate the time evolution of  $\langle \psi(t, \mathbf{x}_1) \dots \psi(t, \mathbf{x}_{2n}) \rangle$  including  $\hbar$  and most desirably in a non-perturbative fashion.

There is a Lagrangian and therefore an action for  $\psi$  from which SPE follow from the variational principle [33]. Therefore one might take the route of [52] and integrate the nonperturbative renormalisation group flow with time as flow parameter [53]. Another possibility would be to explore the fact that  $\hbar$  corresponds to the phase space resolution and thus might be used as a flow parameter with interpretation of Kadanoff's block spin transformation [54].

It might also be possible to interpret the formation of wiggly phases via phase jumps, see Figs. 3 and 4, as something akin to a phase transition. Halo formation under time evolution would then correspond to magnetic domain formation or hadronisation in a ferromagnet or quark-gluon plasma, respectively, under adiabatic cooling.

The ScM could also be connected to effective field theory formulations of LSS formation [48, 55, 56]. Since ScM is a UV complete theory it might be possible to derive an effective field theory including its parameters.

Another research route could be to look for stationary complex solutions of the SPE<sup>3</sup> with the aim of understanding the universality of density profiles of virialised objects. Since ScM allows for virialisation it could prove useful in further analytical understanding of violent relaxation [57, 58] that leads to universal phase space and density profiles [59, 60].

<sup>3</sup> To our knowledge, so far only real solutions have been studied [33, 34]. Fig. 3 however suggests that stationary solutions that result from gravitational collapse are complex.

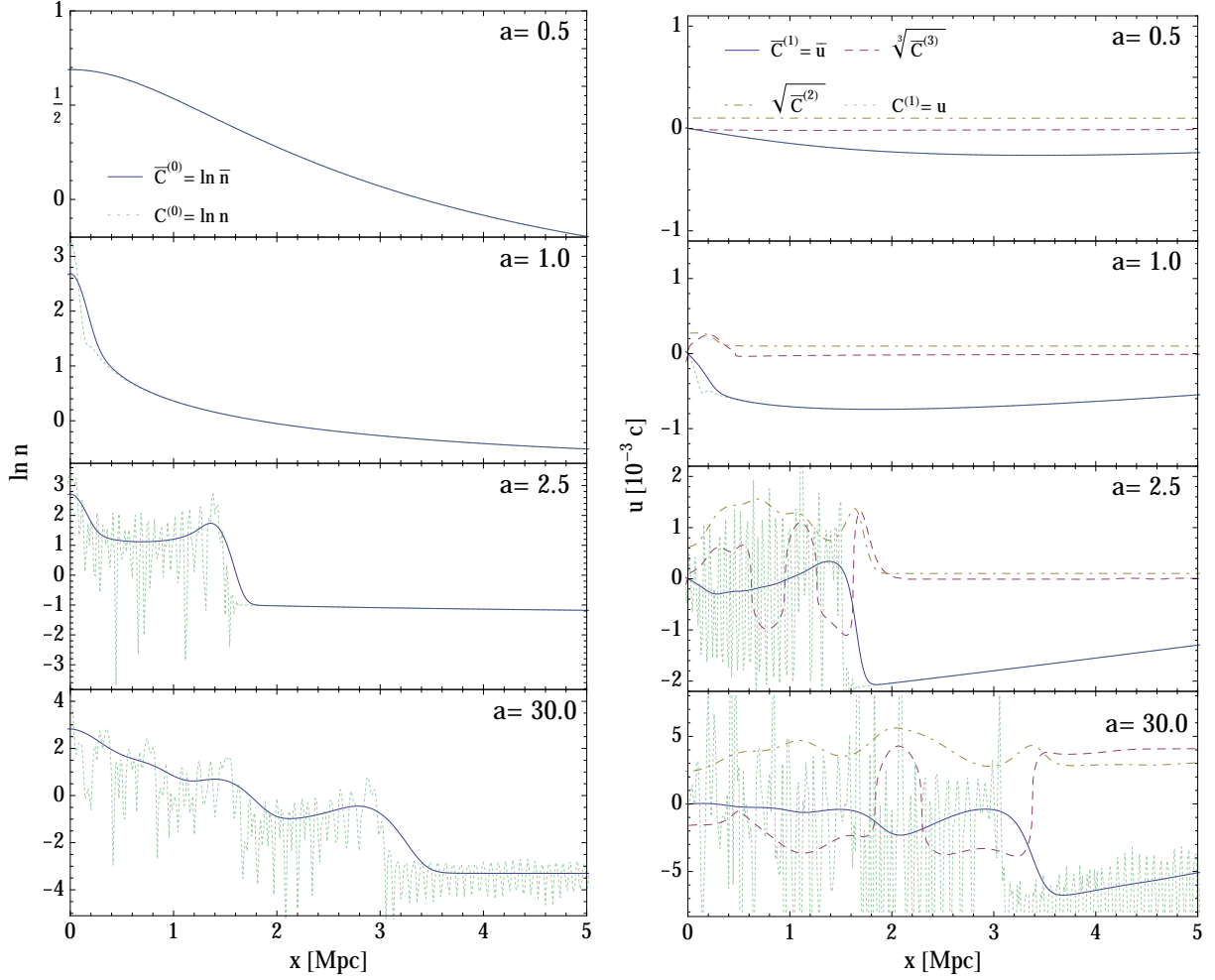


FIG. 7. *left* Number density (*full*) and amplitude of wave function (*dotted*). *right* The first three cumulants and the gradient of phase  $\phi$  of the wave function.

## VI. CONCLUSION

We started with the coupled nonlinear Vlasov-Poisson system Eqs. (6) for the phase-space distribution function  $f$  which is relevant for LSS formation of CDM particles which interact only by means of the gravitational potential. Inspired by the Schrödinger method (ScM) proposed in [22] for numerical simulations we aimed at employing its ability to describe effects of multi-streaming while including recent studies regarding coarse-grained descriptions of CDM and their implications investigated in [17, 61].

Following closely [22], we introduced a complex field  $\psi$  whose time-evolution is governed by the Schrödinger-Poisson equation (SPE) (13) and built the coarse-grained Wigner probability distribution  $\tilde{f}_W$  according to (21) from this wavefunction. We derived that the time-evolution of  $\tilde{f}_W$  is determined by Eq. (22) which is in good correspondence to the one governed by the coarse-grained Vlasov equation (12). Furthermore using a numerical toy example we show how the ScM is able to regularise shell-crossing singularities and accordingly

allows to calculate higher cumulants like velocity dispersion directly from density and velocity and that the dynamics can be followed into the fully nonlinear regime. Furthermore a vorticity is generated by the coarse-graining procedure which can be calculated easily.

We derived the corresponding closed-form fluid-like equations (45) for the smooth density field  $\bar{n}$  and the mass-weighted velocity  $\bar{v}$ . We were able to show that solving these equations means closing the corresponding hierarchy for the moments of  $\tilde{f}_W$ , without truncating the cumulant hierarchy, thereby proposing a different approach to the closure problem than truncation in terms of cumulants. A particular advantage of this approach is that the ‘quantum pressure’ term proportional to  $\hbar^2$  resolves shell-crossing singularities already on the microscopic level. This means that it suffices to solve the SPE (13) and separate the result obtained for  $\psi = \sqrt{n} \exp(i\phi/\hbar)$  into Madelung form, and then simply coarse-grain  $n$  and  $n \nabla \phi$  to obtain the physical density  $\bar{n}$  and momentum  $m \bar{n} \bar{u}$ , respectively. In a similar fashion all higher cumulants (27c) following from (40) can be obtained from a solution to SPE (13).

## ACKNOWLEDGEMENT

We would like to thank Dennis Schimmel for enlightening discussions and comments on the draft. The work of MK &

CU was supported by the DFG cluster of excellence “Origin and Structure of the Universe”. The work of TH was supported by TR33 “The Dark Universe”.

- 
- [1] P. J. E. Peebles, *The large-scale structure of the universe* (1980).
- [2] V. Springel, S. D. M. White, A. Jenkins, C. S. Frenk, N. Yoshida, L. Gao, J. Navarro, R. Thacker, D. Croton, J. Helly, J. A. Peacock, S. Cole, P. Thomas, H. Couchman, A. Evrard, J. Colberg, and F. Pearce, *Nature (London)* **435**, 629 (2005), [astro-ph/0504097](#).
- [3] E. Tempel, R. S. Stoica, V. J. Martínez, L. J. Liivamägi, G. Castellan, and E. Saar, *Mon. Not. R. Astron. Soc.* **438**, 3465 (2014), [arXiv:1308.2533 \[astro-ph.CO\]](#).
- [4] N. E. Chisari and M. Zaldarriaga, *Phys. Rev. D* **83**, 123505 (2011), [arXiv:1101.3555 \[astro-ph.CO\]](#).
- [5] S. R. Green and R. M. Wald, *Phys. Rev. D* **85**, 063512 (2012), [arXiv:1111.2997 \[gr-qc\]](#).
- [6] M. Kopp, C. Uhlemann, and T. Haugg, ArXiv e-prints (2013), [arXiv:1312.3638 \[astro-ph.CO\]](#).
- [7] I. H. Gilbert, *Astrophys. J.* **152**, 1043 (1968).
- [8] R. Teyssier, *Astron. Astrophys.* **385**, 337 (2002), [astro-ph/0111367](#).
- [9] V. Springel, C. S. Frenk, and S. D. M. White, *Nature (London)* **440**, 1137 (2006), [astro-ph/0604561](#).
- [10] M. Boylan-Kolchin, V. Springel, S. D. M. White, A. Jenkins, and G. Lemson, *Mon. Not. R. Astron. Soc.* **398**, 1150 (2009), [arXiv:0903.3041 \[astro-ph.CO\]](#).
- [11] T. Abel, O. Hahn, and R. Kaehler, *Mon. Not. R. Astron. Soc.* **427**, 61 (2012), [arXiv:1111.3944 \[astro-ph.CO\]](#).
- [12] O. Hahn, T. Abel, and R. Kaehler, *Mon. Not. R. Astron. Soc.* **434**, 1171 (2013), [arXiv:1210.6652 \[astro-ph.CO\]](#).
- [13] F. Bernardeau, S. Colombi, E. Gaztañaga, and R. Scoccimarro, *Phys. Rep.* **367**, 1 (2002), [astro-ph/0112551](#).
- [14] T. Buchert, A. L. Melott, and A. G. Weiss, *Astron. Astrophys.* **288**, 349 (1994), [astro-ph/9309056](#).
- [15] S. N. Gurbatov, A. I. Saichev, and S. F. Shandarin, *Mon. Not. R. Astron. Soc.* **236**, 385 (1989).
- [16] D. H. Weinberg and J. E. Gunn, *Mon. Not. R. Astron. Soc.* **247**, 260 (1990).
- [17] A. Dominguez, *Phys. Rev. D* **62**, 103501 (2000).
- [18] T. Buchert and A. Domínguez, *Astron. Astrophys.* **438**, 443 (2005), [astro-ph/0502318](#).
- [19] M. Pietroni, G. Mangano, N. Saviano, and M. Viel, *J. Cosmol. Astropart. Phys.* **1**, 019 (2012), [arXiv:1108.5203 \[astro-ph.CO\]](#).
- [20] S. Pueblas and R. Scoccimarro, *Phys. Rev. D* **80**, 043504 (2009), [arXiv:0809.4606 \[astro-ph\]](#).
- [21] Y. B. Zel’dovich, *Astron. Astrophys.* **5**, 84 (1970).
- [22] L. M. Widrow and N. Kaiser, *Astrophys. J. Letters* **416**, L71 (1993).
- [23] G. Davies and L. M. Widrow, ArXiv Astrophysics e-prints (1996), [astro-ph/9607133](#).
- [24] P. Coles and K. Spencer, *Mon. Not. Roy. Astron. Soc.* **342**, 176 (2003), [arXiv:astro-ph/0212433 \[astro-ph\]](#).
- [25] C. J. Short and P. Coles, *J. Cosmol. Astropart. Phys.* **12**, 012 (2006), [astro-ph/0605012](#).
- [26] D. Committee, R. Larimore, and R. L. Guenther, “A numerical study of the time dependent schrödinger equation coupled with newtonian gravity,” (1995).
- [27] K. Husimi, *Nippon Sugaku-Buturigakkwai Kizi Dai 3 Ki* **22**, 264 (1940).
- [28] K. Takahashi, *Progress of Theoretical Physics Supplement* **98**, 109 (1989).
- [29] L. M. Widrow, *Phys. Rev. D* **55**, 5997 (1997), [astro-ph/9607124](#).
- [30] D. Giulini and A. Großardt, *Classical and Quantum Gravity* **29**, 215010 (2012), [arXiv:1206.4250 \[gr-qc\]](#).
- [31] J. Rogel-Salazar, *European Journal of Physics* **34**, 247 (2013), [arXiv:1301.2073 \[cond-mat.quant-gas\]](#).
- [32] E. H. Lieb, *Studies in Applied Mathematics* **57**, 93 (1977).
- [33] E. R. Arriola and J. Soler, *Journal of Statistical Physics* **103**, 1069 (2001).
- [34] D. M. Moroz, R. Penrose, and P. Tod, *Classical and Quantum Gravity* **15**, 2733 (1998).
- [35] E. Madelung, *Zeitschrift für Physik* **40**, 322 (1927).
- [36] E. A. Spiegel, *Physica D Nonlinear Phenomena* **1**, 236 (1980).
- [37] E. Thomson, *Schrödinger Wave-mechanics and Large Scale Structure* (University of Glasgow, 2011).
- [38] R. Johnston, A. N. Lasenby, and M. P. Hobson, ArXiv e-prints (2009), [arXiv:0904.0611 \[astro-ph.CO\]](#).
- [39] E. Tigrak, R. van de Weygaert, and B. J. T. Jones, *Journal of Physics Conference Series* **283**, 012039 (2011).
- [40] M. Schaller, C. Becker, O. Ruchayskiy, A. Boyarsky, and M. Shaposhnikov, ArXiv e-prints (2013), [arXiv:1310.5102 \[astro-ph.CO\]](#).
- [41] Y. L. Klimontovich, *Journal of Plasma Physics* **3**, 148 (1969).
- [42] E. Bertschinger, (1993), [arXiv:astro-ph/9503125 \[astro-ph\]](#).
- [43] K. Morawetz and R. Walke, *Physica A* **330**, 469 (2003).
- [44] E. Wigner, *Phys. Rev.* **40**, 749 (1932).
- [45] N. Cartwright, *Physica A: Statistical Mechanics and its Applications* **83**, 210 (1975).
- [46] R. T. Skodje, H. W. Rohrs, and J. VanBuskirk, *Phys. Rev. A* **40**, 2894 (1989).
- [47] L. Mercolli and E. Pajer, (2013), [arXiv:1307.3220 \[astro-ph.CO\]](#).
- [48] D. Baumann, A. Nicolis, L. Senatore, and M. Zaldarriaga, *JCAP* **1207**, 051 (2012), [arXiv:1004.2488 \[astro-ph.CO\]](#).
- [49] A. A. Klypin and S. F. Shandarin, *Mon. Not. R. Astron. Soc.* **204**, 891 (1983).
- [50] J. Binney and S. Tremaine, *Galactic Dynamics*, chapter 4.8.3, 2nd ed., Princeton Series in Astrophysics (Princeton University Press, 2008).
- [51] T. Haugg, M. Kopp, and C. Uhlemann, “In preparation” (2014).
- [52] S. V. Tassev, *J. Cosmol. Astropart. Phys.* **10**, 022 (2011), [arXiv:1012.0282 \[astro-ph.CO\]](#).
- [53] T. Gasenzer, S. Keßler, and J. M. Pawłowski, *European Physical Journal C* **70**, 423 (2010), [arXiv:1003.4163 \[cond-mat.quant-gas\]](#).
- [54] L. P. Kadanoff, *Physics* **2**, 263 (1966).
- [55] R. A. Porto, L. Senatore, and M. Zaldarriaga, ArXiv e-prints (2013), [arXiv:1311.2168 \[astro-ph.CO\]](#).
- [56] S. M. Carroll, S. Leichenauer, and J. Pollack, ArXiv e-prints (2013), [arXiv:1310.2920 \[hep-th\]](#).

- [57] D. Lynden-Bell, Mon. Not. R. Astron. Soc. **136**, 101 (1967).  
 [58] D. N. Spergel and L. Hernquist, *Astrophys. J. Letters* **397**, L75 (1992).  
 [59] J. F. Navarro, C. S. Frenk, and S. D. M. White, *Astrophys. J.* **490**, 493 (1997), [astro-ph/9611107](#).  
 [60] A. A. Dutton and A. V. Macciò, ArXiv e-prints (2014), [arXiv:1402.7073 \[astro-ph.CO\]](#).  
 [61] M. Pietroni, G. Mangano, N. Saviano, and M. Viel, *JCAP* **1201**, 019 (2012), [arXiv:1108.5203 \[astro-ph.CO\]](#).  
 [62] C. Rampf and T. Buchert, *J. Cosmol. Astropart. Phys.* **6**, 021 (2012), [arXiv:1203.4260 \[astro-ph.CO\]](#).

### Appendix A: Explicit calculation for closing the hierarchy

As mentioned in [III C 3](#) it can be shown that the evolution equation for the second moment (46) is automatically fulfilled when the coarse-grained fluid equations (45) for density  $\bar{n}$  and mass-weighted peculiar velocity  $\bar{v}$  are satisfied. In order to prove that we perform the following steps:

1. Start with the time evolution equation for the second moment (46) which involves the third one.

$$\partial_t \bar{M}_{ij}^{(2)} \stackrel{?}{=} -\frac{1}{a^2 m} \nabla_k \bar{M}_{ijk}^{(3)} - m \nabla_{(i} \bar{V} \exp(\sigma_x^2 \overleftarrow{\nabla}_x \overrightarrow{\nabla}_x) (\bar{n} \bar{u}_{j)}) + \frac{\sigma_p^2}{a^2} (\bar{n} \bar{u}_{(i),j)}) \quad (\text{A1})$$

2. Insert the explicit expressions for  $\bar{M}^{(2)}$  and  $\bar{M}^{(3)}$  given by (41c) and (41d).

$$\begin{aligned} \partial_t \exp\left(\frac{\sigma_x^2}{2} \Delta\right) \left[ n \phi_{,i} \phi_{,j} + \sigma_p^2 n \delta_{ij} + \frac{\hbar^2}{4} \left( \frac{n_{,i} n_{,j}}{n} - n_{,ij} \right) \right] \\ \stackrel{?}{=} -\exp\left(\frac{\sigma_x^2}{2} \Delta\right) \nabla_k \left\{ n \phi_{,i} \phi_{,j} \phi_{,k} + \sigma_p^2 \delta_{ij} n \phi_{,k} + \frac{\hbar^2}{4} \left[ \left( \frac{n_{,i} n_{,j}}{n} - n_{,ij} \right) \phi_{,k} - n \phi_{,ijk} \right] \right\} \\ - \nabla_{(i} \bar{V} \exp(\sigma_x^2 \overleftarrow{\nabla}_x \overrightarrow{\nabla}_x) (\bar{n} \bar{u}_{j)}) + \sigma_p^2 (\bar{n} \bar{u}_{(i),j)}) \end{aligned} \quad (\text{A2})$$

3. Express everything in terms of  $\bar{n}$  and  $\bar{u}_i = (\overline{n \phi_{,i}})/\bar{n}$  using the rule for the  $D$ -symbol (42).

$$\begin{aligned} \partial_t \left\{ \exp\left[\frac{\sigma_x^2}{2} (\Delta - D)\right] \left[ \frac{(\bar{n} \bar{u}_i)(\bar{n} \bar{u}_j)}{\bar{n}} + \frac{\hbar^2}{4} \left( \frac{\bar{n}_{,i} \bar{n}_{,j}}{\bar{n}} - \bar{n}_{,ij} \right) \right] + \sigma_p^2 \bar{n} \delta_{ij} \right\} \\ \stackrel{?}{=} -\exp\left[\frac{\sigma_x^2}{2} (\Delta - D)\right] \nabla_k \left[ \frac{(\bar{n} \bar{u}_i)(\bar{n} \bar{u}_j)(\bar{n} \bar{u}_k)}{\bar{n}^2} + \frac{\hbar^2}{4} \left[ \left( \frac{\bar{n}_{,i} \bar{n}_{,j}}{\bar{n}} - \bar{n}_{,ij} \right) \frac{\bar{n} \bar{u}_k}{\bar{n}} - \frac{1}{3} \bar{n} \left( \frac{\bar{n} \bar{u}_i}{\bar{n}} \right)_{,jk} \right] \right] \\ - \sigma_p^2 \nabla_k \left( \delta_{ij} \bar{n} \bar{u}_k \right) - \nabla_{(i} \bar{V} \exp(\sigma_x^2 \overleftarrow{\nabla}_x \overrightarrow{\nabla}_x) (\bar{n} \bar{u}_{j)}) + \sigma_p^2 (\bar{n} \bar{u}_{(i),j)}) \end{aligned} \quad (\text{A3})$$

4. Pull the time-derivative through the smoothing operator and apply the product rule to re-express the terms.

$$\begin{aligned} \exp\left[\frac{\sigma_x^2}{2} (\Delta - D)\right] \left\{ \frac{\partial_t (\bar{n} \bar{u}_i)(\bar{n} \bar{u}_j)}{\bar{n}} - \frac{(\bar{n} \bar{u}_i)(\bar{n} \bar{u}_j) \partial_t \bar{n}}{\bar{n}^2} + \frac{\hbar^2}{4} \left( \frac{\partial_t \bar{n}_{,i} \bar{n}_{,j}}{\bar{n}} - \frac{\partial_t \bar{n} \bar{n}_{,i} \bar{n}_{,j}}{\bar{n}^2} - \partial_t \bar{n}_{,ij} \right) \right\} + \sigma_p^2 \partial_t \bar{n} \delta_{ij} \\ \stackrel{?}{=} \exp\left[\frac{\sigma_x^2}{2} (\Delta - D)\right] \left\{ -\nabla_k \left( \frac{\bar{n} \bar{u}_i \bar{n} \bar{u}_k}{\bar{n}} \right) \frac{\bar{n} \bar{u}_j}{\bar{n}} - \frac{\bar{n} \bar{u}_i \bar{n} \bar{u}_k}{\bar{n}} \nabla_k \left( \frac{\bar{n} \bar{u}_j}{\bar{n}} \right) - \nabla_{(i} \bar{V} (\bar{n} \bar{u}_{j)}) - \frac{\hbar^2}{4} \nabla_k \left[ \left( \frac{\bar{n}_{,i} \bar{n}_{,j}}{\bar{n}} - \bar{n}_{,ij} \right) \frac{\bar{n} \bar{u}_k}{\bar{n}} - \frac{1}{3} \bar{n} \left( \frac{\bar{n} \bar{u}_i}{\bar{n}} \right)_{,jk} \right] \right\} \\ - \sigma_p^2 \nabla_k (\bar{n} \bar{u}_k) \delta_{ij} \end{aligned} \quad (\text{A4})$$

5. Employ the fluid equations (45) to carry out the time derivatives  $\partial_t(\bar{n})$  and  $\partial_t(\bar{n} \bar{u}_i)$ .

$$\begin{aligned} \exp\left[\frac{\sigma_x^2}{2} (\Delta - D)\right] \left\{ -\exp\left[\frac{\sigma_x^2}{2} (\Delta - D)\right] \left[ \nabla_k \left( \frac{\bar{n} \bar{u}_i \bar{n} \bar{u}_{(i)}}{\bar{n}} \right) + \nabla_{(i} \bar{V} \bar{n} + \frac{\hbar^2}{4} \nabla_k \left( \frac{\bar{n}_{,k} \bar{n}_{,i}}{\bar{n}} - \bar{n}_{,ki} \right) \right] \frac{\bar{n} \bar{u}_{j)}}{\bar{n}} + \frac{\bar{n} \bar{u}_i \bar{n} \bar{u}_j (\bar{n} \bar{u}_k)_{,k}}{\bar{n}^2} \right. \\ \left. - \frac{\hbar^2}{4} \left( \frac{(\bar{n} \bar{u}_k)_{,k(i} \bar{n}_{,j)}}{\bar{n}} - \frac{(\bar{n} \bar{u}_k)_{,k} \bar{n}_{,i} \bar{n}_{,j}}{\bar{n}^2} - (\bar{n} \bar{u}_k)_{,ijk} \right) \right\} \\ \stackrel{?}{=} \exp\left[\frac{\sigma_x^2}{2} (\Delta - D)\right] \left\{ -\nabla_k \left( \frac{\bar{n} \bar{u}_i \bar{n} \bar{u}_k}{\bar{n}} \right) \frac{\bar{n} \bar{u}_j}{\bar{n}} - \frac{\bar{n} \bar{u}_i \bar{n} \bar{u}_k}{\bar{n}} \nabla_k \left( \frac{\bar{n} \bar{u}_j}{\bar{n}} \right) - \nabla_{(i} \bar{V} (\bar{n} \bar{u}_{j)}) - \frac{\hbar^2}{4} \nabla_k \left[ \left( \frac{\bar{n}_{,i} \bar{n}_{,j}}{\bar{n}} - \bar{n}_{,ij} \right) \frac{\bar{n} \bar{u}_k}{\bar{n}} - \frac{1}{3} \bar{n} \left( \frac{\bar{n} \bar{u}_i}{\bar{n}} \right)_{,jk} \right] \right\} \end{aligned} \quad (\text{A5})$$

6. Combine the different  $D$ -symbols acting successively on the terms to yield an overall  $D$ -symbol according to

$$\exp\left[\frac{1}{2}\sigma_x^2(\Delta - D_{ABC})\right](\bar{A}\bar{B}\bar{C}) = \exp\left[\frac{1}{2}\sigma_x^2(\Delta - D_{A(BC)})\right]\left[\bar{A}\exp\left[\frac{1}{2}\sigma_x^2(\Delta - D_{BC})\right](\bar{B}\bar{C})\right].$$

This is possible since the action of the  $D$ -symbol depends on the product structure it is acting on.

$$\begin{aligned} & \exp\left[\frac{\sigma_x^2}{2}(\Delta - D)\right]\left\{\frac{\hbar^2}{4}\left[\nabla_k\left(\frac{\bar{n}_{,k}\bar{n}_{,i}}{\bar{n}} - \bar{n}_{,k(i)}\right)\frac{\bar{n}\bar{u}_{j)}}{\bar{n}} + \frac{(\bar{n}\bar{u}_k)_{,k(i)}\bar{n}_{,j}}{\bar{n}} - \frac{(\bar{n}\bar{u}_k)_{,k}\bar{n}_{,i}\bar{n}_{,j}}{\bar{n}^2} - (\bar{n}\bar{u}_k)_{,ijk}\right]\right\} \\ & \stackrel{\text{cyc. perm.}}{=} \exp\left[\frac{\sigma_x^2}{2}(\Delta - D)\right]\left\{\frac{\hbar^2}{4}\nabla_k\left[\left(\frac{\bar{n}_{,i}\bar{n}_{,j}}{\bar{n}} - \bar{n}_{,ij}\right)\frac{\bar{n}\bar{u}_k}{\bar{n}} - \frac{1}{3}\bar{n}\left(\frac{\bar{n}\bar{u}_i}{\bar{n}}\right)_{,jk}\right]\right\} \end{aligned} \quad (\text{A6})$$

One has to note that equality is only established once we make use of the constraint Eq. (45c).

## Appendix B: Lagrangian formulation

We follow [62] to rewrite the fluid-like system Eqs. (15) formulated in terms  $n$  and  $\nabla\phi$  evaluated at the Eulerian position  $\mathbf{x}$ , into a Lagrangian system in which the sole dynamical variable is the displacement field  $\Psi$ , that maps between  $\mathbf{x}$  and the Lagrangian (or initial coordinate of a fluid element)  $\mathbf{q}$ . Since the continuity and Euler equation Eqs. (9) are unchanged apart from the added quantum potential  $Q$  in Eq. (15b) the analogue of Eq. 2.31 in [62] is

$$\begin{aligned} & \left[(1 + \Psi_{,l,l})\delta_{ij} - \Psi_{,i,j} + \Psi_{,i,j}^c\right]\Psi_{,i,j}'' = \\ & \alpha(\eta)(J^F - 1) + J^F \frac{\hbar^2}{4m^2} \Delta_x \left( \frac{\Delta_x[(J^F)^{-1/2}]}{(J^F)^{-1/2}} \right), \end{aligned} \quad (\text{B1})$$

which can be obtained by solving the continuity equation with  $1 + \delta = 1/J^F$ , where  $J^F = \det(F_{ij}) = \det(\delta_{i,j} + \Psi_{,i,j})$  and  $F_{ij} = \partial x^i / \partial q^j$  is the Jacobian relating  $\mathbf{x}$  and  $\mathbf{q}$  and with  $\nabla_x \phi / m = \Psi'$ , where a prime denotes a derivative wrt to superconformal time  $\eta$  related to cosmic time  $t$  and conformal time  $\tau$  via  $dt = a^2 d\eta = a d\tau$ . In eq. (B1) the Laplacians are with respect to  $\mathbf{x}$ , rather than  $\mathbf{q}$  and have therefore to be rewritten in terms of  $\mathbf{q}$  using the Jacobian  $F_{ij}$ . The equation is supplemented by a constraint equation  $F_{i,n} \epsilon_{njk} F_{l,j} F_{l,k}^t = 0$  that follows from  $\nabla_x \times \mathbf{u} = 0$ . If the density and velocity distribution depend only on  $\mathbf{x} = (x, 0, 0)$ , (and therefore  $\mathbf{q} = (q, 0, 0)$ ), the above system can be written, using  $\epsilon_{qqq} = 0$  and  $\Psi_i =: \Psi \delta_{iq}$  and  $J^F = 1 + \Psi_{,q}$  as

$$\Psi'' = \alpha(\eta)\Psi + \frac{\hbar^2}{2m^2} \left( \frac{10(\Psi_{,qq})^3}{(1 + \Psi_{,q})^6} - 8 \frac{\Psi_{,qq}\Psi_{,qqq}}{(1 + \Psi_{,q})^5} + \frac{\Psi_{,qqqq}}{(1 + \Psi_{,q})^4} \right), \quad (\text{B2})$$

where  $\alpha(\eta) = 4\pi G a \rho_0$ . Note that compared to the 3D case (B1), we were able to integrate already once over  $q$  in order to obtain (B2).

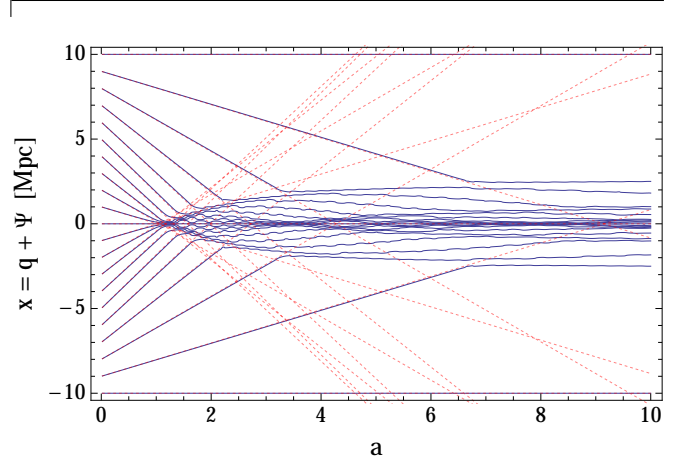


FIG. 8. red dotted Zel'dovich trajectories Eq. (B3), blue Bohmian trajectories Eq. (B2).

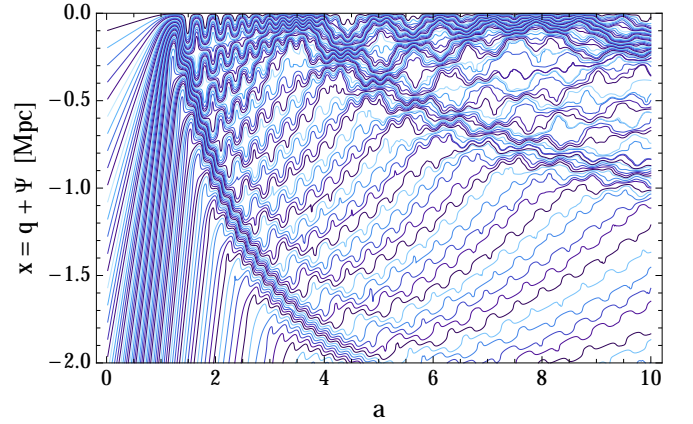


FIG. 9. Detailed view of the Bohmian trajectories, Eq. (B2).

In the case of  $\hbar = 0$ , we recover the case of dust

$$\Psi_d'' = \alpha(\eta)\Psi_d, \quad (\text{B3})$$

whose exact solution is the Zel'dovich approximation  $\Psi_{,q}(\mathbf{q}, a) = -D(a)\delta_{\text{lin}}(\mathbf{x} = \mathbf{q})$ , where  $\delta_{\text{lin}}(\mathbf{x})$  is the initial con-



dition Eulerian density field (which is assumed to vanish at  $a = 0$ ) linearly extrapolated to  $a = 1$  using the linear growth  $D(a)$ . The red dashed lines in Fig. 1 are points  $(q + \Psi, \Psi')$ , parametrized by  $q$  and can be extended after shell crossing. Unfortunately, this continuation does not behave as CDM and the trajectories continue on their straight lines indefinitely, see red lines in (B2). Including the  $\hbar$ -terms, a separation ansatz does not work anymore and we do not expect to find an exact solution of (B2), see Figs. 8 and 9 for the complicated dynamics of  $\Psi$  for the case of initial conditions studied in Sec. IV. Under a coarse grained view the Bohmian and collisionless CDM trajectories would turn into network that is indistinguishable. On a microscopic level though, they are very different, see Fig. (9). Although the phase space density  $f_H$  behaves as if shell crossings and multi-stream regions form, the phase  $\phi$  of the wave function  $\psi$  is single valued and

therefore the trajectories  $\mathbf{q} + \Psi$  never intersect. The intricate behaviour of  $\Psi$  *emulates* multi-streaming. Given the Bohmian trajectories  $\Psi(\mathbf{q}, a)$  one can recover  $n(\mathbf{x}, a)$  and  $\phi(\mathbf{x}, a)$  via

$$n(x, a) = \frac{1}{1 + \Psi_{,q}(q, a)} \Big|_{q=q(x,a)} \quad (\text{B4})$$

$$\partial_x \phi(x, a)/m = \Psi'(q, a) \Big|_{q=q(x,a)}, \quad (\text{B5})$$

where the  $q$ -dependent expressions are converted into  $x$ -depend ones via inversion of  $x = q + \Psi(q, a)$ . The Lagrangian formulation Eq. (B1) of the Madelung representation, Eq. (14) suffers from the same singularities as the Euler-type equation Eq. (15b); at the isolated space-time points where the phase  $\phi$  jumps about  $2\pi$ , the velocity  $\nabla\phi$  and therefore  $\dot{\Psi}$  diverge and change sign. Figs. 8 and 9 were constructed from the solution of the Schrödinger-Poisson equation (13) and not from Eq. (B2).